# Modelling and Simulation of MEMS Beam-Type Switches with Dielectric Interfaces and Geometrical Variations

A DISSERTATION

SUBMITTED IN PARTIAL FULFILLMENT OF THE REQUIREMENTS
FOR THE AWARD OF THE DEGREE
OF

MASTER OF TECHNOLOGY
IN
**COMPUTER AIDED ANALYSIS AND DESIGN**


Submitted by:

**ANUPAM KIMOTHI**

**(2023/CAD/05)**

Under the supervision of

**Prof. VIJAY GAUTAM**




**DEPARTMENT OF MECHANICAL ENGINEERING**
**DELHI TECHNOLOGICAL UNIVERSITY**
(Formerly Delhi College of Engineering)
Bawana Road, Delhi-110042


**MAY, 2025**

**DELHI TECHNOLOGICAL UNIVERSITY**
(Formerly Delhi College of Engineering)
Bawana Road, Delhi-110042

# CANDIDATE DECLARATION

I, ANUPAM KIMOTHI, Roll No. 2023/CAD/05 student of MTech-Computer Aided Analysis and Design, hereby declare that the project Dissertation titled "Modelling and Simulation of MEMS Beam-Type Switches with Dielectric Interfaces and Geometrical Variations" which is submitted by me to the Department of Mechanical Engineering, Delhi Technological University, Delhi in partial fulfilment of the requirement for the award of the degree of Master of Technology, is original and not copied from any source without proper citation. This work has not previously formed the basis for the award of any Degree, Diploma Associateship, Fellowship or other similar title or recognition.

Place: Delhi

Date: **ANUPAM KIMOTHI**

**DEPARTMENT OF MECHANICAL ENGINEERING**
DELHI TECHNOLOGICAL UNIVERSITY
(Formerly Delhi College of Engineering)
Bawana Road, Delhi-110042

# CERTIFICATE

I hereby certify that the Project Dissertation titled "Modelling and Simulation of MEMS Beam-Type Switches with Dielectric Interfaces and Geometrical Variations" which is submitted by **Anupam Kimothi**, Roll No. **2023/CAD/05**, Department of Mechanical Engineering, Delhi Technological University, Delhi in partial fulfilment of the requirement for the award of the degree of Master of Technology, is a record of the project work carried out by the students under my supervision. To the best of knowledge this work has not been submitted in part or full for any Degree or Diploma to this University or elsewhere.

Place: Delhi
Date:

**Dr. VIJAY GAUTAM**
**Professor**
**SUPERVISOR**

# ABSTRACT

Low power consumption, great isolation, and fast switching capability of microelectromechanical systems beam-type capacitive switches have made them interesting components in various radio frequency and microwave applications. The modelling, simulation, and analysis of MEMS cantilever beam capacitive switches including dielectric interfaces is presented in this thesis in its whole. The aim of this work is to investigate the effects on the electromechanical performance of switches of geometric parameters, dielectric layers, and electrode layouts.

Considering beam dimensions, electrode area, air gap, and the presence of a dielectric layer, an analytical model for pull-in voltage was developed offering a theoretical foundation for design optimisation. Four different cases varying beam length, width, dielectric presence, and electrode size were investigated tip displacement, pull-in voltage, electric field distribution, and stress concentration using COMSOL Multiphysics by means of detailed finite element simulations.

Larger beams with dielectric layers show reduced pull-in voltages due to modified electric field distribution and effective gap reduction; smaller beams show increased pull-in voltages and higher von Mises stress, so indicating greater mechanical constraints. The electric field study shows enhanced field localisation at dielectric interfaces, so influencing device dependability. Under less than 6% error, comparison of simulation results with analytical predictions reveals good agreement, so verifying the modelling technique.

This work illustrated important trade-offs of device miniaturization, operating voltage and mechanical reliability that provided a rich framework to think about designing and

fabricating MEMS switches. These findings create a path for bettering MEMS technology to use for safe, low-power RF switching for real-world usage and the techniques we have developed could provide a strong methodology to improve devices in the oscillators and near-ideal RF CA filter space.

# ACKNOWLEDGEMENT

I would like to express my sincere gratitude to my guide, **Prof. Vijay Gautam**, Professor in the Department of Mechanical Engineering and **Dr. Ankur Gupta,** Professor in the Centre of Applied Research in Electronics IIT Delhi**,** for his invaluable guidance, support, and expertise throughout the course of this research project. His constant encouragement, insightful feedback, and dedication have been instrumental in shaping the direction and progress of this work. His deep knowledge and passion for the subject have inspired me to strive for excellence and explore new avenues in the field of Micro Electro Mechanical switches.

I would also like to extend my heartfelt appreciation to **Prof. B. B. Arora**, Head of the Department of Mechanical Engineering, for his support and encouragement. His vision and leadership have provided a conducive environment for academic and research pursuits. I am grateful for his valuable insights and guidance that have contributed to the overall success of this project.

Lastly, I would like to acknowledge my family and friends for their unwavering support, encouragement, and understanding throughout this research endeavour. Their love, belief in my abilities, and motivation have been the driving force behind my perseverance and determination.

**ANUPAM KIMOTHI**
23/CAD/05
MTech (Computer Aided Analysis and Design)
Delhi Technological University

# TABLE OF CONTENTS

# LIST OF TABLES

# LIST OF FIGURES

# NOMENCLATURE

| | |
|---|---|
| B | Beam width (m) |
| E | Young's Modulus of the beam material (Pa) |
| Fe | Electrostatic pressure per unit area ($N/m^2$) |
| g0 | Initial air gap between beam and electrode (m) |
| H | Beam thickness (m) |
| I | Moment of inertia ($m^4$) |
| Keq | Equivalent spring constant of the cantilever beam (N/m) |
| L | Length of the cantilever beam (m) |
| M | Bending moment (Nm) |
| q(x) | Distributed electrostatic load per unit length (N/m) |
| σ | Bending stress (Pa) |
| td | Thickness of dielectric layer (m) |
| V | Applied voltage (V) |
| Vpi | Pull-in voltage (V) |
| w | Local deflection of the beam (m) |
| y | Distance from neutral axis (m) |
| εo | Permittivity of free space (F/m) |
| εr | Relative permittivity of the dielectric |

# CHAPTER 1

# INTRODUCTION

## 1.1 Background

Microelectromechanical systems (MEMS) technology has allowed the microscale integration of mechanical components and electrical circuits opening new possibilities for small, high-performance devices across many sectors including telecommunications, biomedical sensing, aerospace, and consumer electronics. Usually MEMS devices consist of microscale beams, cantilevers, membranes, or plates responding to electrical, mechanical, thermal, or magnetic stimuli.

Among the different kinds of MEMS devices, MEMS switches have drawn a lot of interest as they enable very low power consumption and great isolation features control of electrical signals. MEMS capacitive switches in RF and microwave circuits allow signal switching by electrostatically actuating a moving beam towards a fixed electrode, hence changing the capacitance state. Among low insertion loss, good isolation, excellent linearity, and low power consumption, these switches demonstrate greater performance than solid-state semiconductor switches.

Usually a MEMS capacitive switch consists of a cantilever beam suspended above a fixed bottom electrode split by an air gap. Under a voltage, the electrostatic force pulls the beam towards the electrode until it reaches a critical voltage sometimes referred to as the pull-in voltage. By now the electrostatic force surpasses the mechanical restoring force of the beam, collapsing it onto the electrode and so closing the circuit. The pull-in voltage determines essentially switch power consumption, dependability, and operational lifetime.

Still, the device performance most critically is defined by the mechanical and electrical design parameters: beam geometry (length, width, thickness), electrode size, air gap distance, and dielectric layer presence. Usually made of silicon nitride or silicon dioxide, dielectric layers are sandwiched between the beam and electrode to prevent direct electrical contact and reduce contact wear, hence increasing switch lifespan. These layers affect the effective gap and electric field distribution, therefore impacting pull-in voltage and switching behaviour.

Moreover, knowing how scaling affects mechanical stress, displacement, and electrostatic forces becomes crucial as MEMS switches are tiny to meet the requirements for small and integrated systems. Since smaller beams run greater stress and could induce possible fatigue, hence raising device failure risk, mechanical dependability is very crucial. Effective modelling of these linked electromechanical processes is necessary to maximise MEMS switch designs. employed voltages allow complete examination of beam deformation, electric field distribution, and stress under numerical methods such the finite element method (FEM), employed in simulation tools such COMSOL Multiphysics. Although they enhance analytical models that provide closed-form solutions, such simulations may oversimplify complex real-world interactions including fringe fields and nonlinear deformations.

This thesis models and simulates both with and without dielectric layers MEMS cantilever beam-type capacitive switches. It looks at how various beam widths and electrode areas impact significant performance criteria including mechanical stress distribution, pull-in voltage, tip displacement, and electric field intensity. Combining simulation findings with analytical models and handling design trade-offs aims to help to produce low-voltage, trustworthy MEMS switches for advanced applications.

### 1.2 Problem Statement

Fast development of wireless communication and sensor technologies calls for MEMS switches with low actuation voltage, great dependability, and miniaturised form sizes. Although MEMS capacitive switches have low power consumption and great RF performance, some difficulties still exist in best designing their practical implementation. The correct prediction and control of the pull-in voltage, which determines the working voltage of the switch, presents one of the difficulties. Among several factors, including beam geometry, electrode size, air gap, and material qualities, the pull-in voltage reflects First-order approximations are given by conventional analytical models, which also frequently ignore nonlinearities resulting from complicated 3D deformation, fringe electric fields, and dielectric layer effects.

Moreover, the inclusion of dielectric layers—which are necessary to prevent stiction and improve durability—introduces still another level of complexity. Dielectric materials change the effective capacitance, mechanical behaviour of the switch, and electric field

distribution. Still, exact quantification of their influence calls for combined Multiphysics modelling.

The mechanical stress within the cantilever beam during operation is yet another important concern. Higher actuation voltages and miniaturisation trends can raise stress concentrations, particularly close to fixed supports, maybe causing mechanical wear or failure. Device lifetime depends on a complete knowledge of stress distribution and its connection with beam size and materials.

Comprehensive simulation studies that simultaneously consider geometric fluctuations, dielectric effects, and coupled electromechanical behaviour are still much needed despite much of study. Such investigations should also verify accuracy and practical relevance by means of validation of simulation results against analytical models. This thesis therefore addresses the following fundamental issues:

• In MEMS cantilever beam capacitive switches, how do beam width and length as well as electrode size affect the pull-in voltage, tip displacement, and stress distribution?

• What is the quantitative effect on the mechanical and electrostatic behaviour of the switch of adding a dielectric layer?

• How closely numerical simulations employing finite element modelling in COMSOL Multiphysics match classical analytical models of MEMS switches?

• When balancing low pull-in voltage needs against mechanical dependability in scaled-down switches, what design trade-offs result?

This work intends to offer useful insights and practical guidance for optimising MEMS switch designs appropriate for low-power, high-reliable applications in modern electronic systems by answering these concerns via a combined simulation and analytical approach.

**1.3 Objectives**

With specific attention on understanding the impact of beam geometry and dielectric layers on their electromechanical performance, the main goal of this work is to fully model, simulate, and analyse MEMS cantilever beam-type capacitive switches. The effort intends to close the gap between simplified analytical models and thorough numerical simulations thereby provide a strong framework for design optimisation. The thesis has as its particular goals these:

- Incorporating realistic material properties (gold for beam and electrode, silicon nitride for the dielectric layer) and geometric configurations, develop a coupled electromechanical finite element model of MEMS beam-type capacitive switches in COMSOL Multiphysics. Under different applied voltages this model will allow modelling of important performance metrics like tip displacement, electric field distribution, pull-in voltage, and structural stress.
- Examine the impact on the pull-in voltage and mechanical behaviour of the switches of changing beam parameters (length and width) and bottom electrode size. Two beam sizes—200 μm x 90 μm and 140 μm x 75 μm—will be investigated to see how mechanical stresses and operational voltage are affected by miniaturising. Comparing examples with and without silicon nitride dielectric layers helps one to quantify the effect of dielectric layers on device performance. This include investigating variations in effective air gap, electric field strengths, pull-in voltages, and stress distributions arising from the dielectric presence.
- Verify the simulation results against standard analytical models of MEMS capacitive switches produced from known beam theory and electrostatics. To evaluate model accuracy and expose limits of analytical approximations, this will include computed pull-in voltages analytically being compared with COMSOL simulation outputs. Under operational conditions, examine the von Mises stress distribution inside the cantilever beams to evaluate mechanical dependability and spot any failure sites. Particularly when the switches are miniaturised and exposed to greater voltages, this is absolutely vital for guaranteeing device durability.
- Design rules and trade-off analysis depending on the outcomes will help to emphasise the harmony between low actuation voltage and mechanical integrity maintenance. These revelations seek to support the useful design of MEMS capacitive switches specifically for low-power, high-performance uses.
- To enable next studies and development, clearly, repeatable documentation and presentation of thorough parametric data including displacement-voltage behaviour, electric field mapping, stress contour plots, and pull-in voltage trends.
- By reaching these goals, the research will help to clarify MEMS capacitive switch design, therefore enabling better device performance and dependability in many different technical applications.

### 1.4 Future and Approach

With specific attention on how geometric factors and dielectric layers affect device performance, the scope of this thesis spans the modelling, simulation, and analysis of MEMS cantilever beam-type capacitive switches. Important electromechanical properties like pull-in voltage, tip displacement, electric field distribution, and structural stress—all of which are fundamental for the design and optimisation of dependable MEMS switches in useful applications—are addressed in this work.

#### 1.4.1 Future:

• The work is limited to beam-type capacitive switches set as cantilever beams, extensively employed in RF MEMS switches because of their simplicity and efficiency. Reflecting usual design modifications, beam dimensions are modified to include two sets: a smaller beam with length 140 μm and breadth 75 μm and a bigger beam with length 200 μm and width 90 μm.

• Both topologies are investigated both with and without a dielectric layer (silicon nitride), therefore enabling study of dielectric impacts on mechanical dependability and electrostatic behaviour.

• Common MEMS materials for this use, silicon nitride as the dielectric and gold for the beam and electrode, limit the material choices.

• Coupled electrostatic-structural issues are solved using COMSOL Multiphysics utilising COMSOL Multiphysics under validation of results by means of analytical models.

• The paper stresses static pull-in voltage and stress analysis; dynamic impacts and temperature fluctuations are outside the current scope but advised for next investigation.

#### 1.4.2 Approach:

- Built in COMSOL, a thorough finite element model of the MEMS switch is built encompassing material properties, geometry, boundary conditions, and applied voltages. Combining mechanical deformation with electrostatic forces allows one to capture the nonlinear behaviour generating pull-in.

- We carefully model several scenarios with altering beam size and dielectric presence to assess their effects on significant performance criteria like tip displacement against voltage characteristics and pull-in voltage thresholds.
- Dielectric layer effects on field concentration and mechanical integrity are assessed using spatial distribution of electric fields and von Mises stress within the beam, therefore providing knowledge of reliability issues.

Validation:

- By means of theoretical pull-in voltages computed using analytical models derived in Chapter 3, subsequently matched against simulation data, the correctness and robustness of the COMSOL model are validated.
- In order to understand the effects of geometry and dielectric layers, results are extensively investigated thus stressing trade-offs between device size, operating voltage, and mechanical stress and so guiding ideal MEMS switch design. This approach establishes a strong base for future advancements and experimental validation and ensures a complete awareness of the physical events regulating MEMS beam-type capacitive switches.

### 1.5 Significance of the Study

This work is important since it systematically studies MEMS beam-type capacitive switches using analytical modelling and high-fidelity Multiphysics simulations. MEMS switches offer minimal power consumption, great isolation, and high switching rates, hence modern radio frequency (RF) systems are constructed on them. Still, mechanical dependability, dielectric layer effects, and large pull-in voltages usually restrict their real utility.

The work addresses these challenges using:

- Build exact analytical models: The work provides significant theoretical insights based on which MEMS switch design is directed by use of pull-in voltage and electromechanical behaviour equations covering the implications of beam shape, electrode area, air gap, and dielectric layers. COMSOL Multiphysics helps one to replicate many configurations including the presence or absence of dielectric layers and variations in beam size, therefore allowing an in-depth understanding of the interaction between electrostatic forces and mechanical deformation. Perfect

prediction of pull-in voltages, displacement profiles, electric field distributions, and stress concentrations is therefore enabled.

- Interchanging Simulations Data with Analytical Models Close agreement between analytical predictions and simulation outcomes (with errors less than 6%) guarantees the dependability of the modelling approach. This validation helps one to depend more on using these models for MEMS switch design and optimisation.
- Underlining design trade-offs: Fundamental for efficient MEMS switch manufacture and operation, the work reveals major trade-offs between mechanical stress, pull-in voltage, and miniaturisation. Smaller beams, for example, show larger pull-in voltages and stress concentrations; hence, even more crucial is proper material selection and shape optimisation.
- Structural integrity determined from analysis of von Mises stress distributions guides design of robust MEMS switches for long-term usage by awareness of various failure modes.
- So enabling the design of reliable, efficient, compact MEMS capacitive switches appropriate for next-generation RF applications, so promoting MEMS switch technology generally by offering a rigorous, proven framework merging theory and simulation.

# CHAPTER 2

# LITRAURE REVIEW

Low power consumption, good isolation, and small size make Micro-Electro-Mechanical Systems (MEMS) beam-type switches essential components in radio frequency (RF) and microwave applications. These switches maximise performance measures like actuation voltage, switching speed, and RF characteristics by means of dielectric interfaces and geometrical changes. Simulating the coupled electromechanical and RF behaviour of these switches is accomplished mostly with COMSOL Multiphysics. Focussing on dielectric interfaces and geometrical changes, this literature review synthesises research articles to investigate developments, obstacles, and simulation approaches pertinent to MEMS beam-type switches.

## 2.1 Foundational Studies on MEMS Beam-Type Switches

Low power consumption, good isolation, and small footprint suitable for applications including 5G and IoT make MEMS beam-type switches—which mix cantilever and fixed-fixed beam configurations—critical components in RF and wireless communication systems [1]. Early pioneering effort by Muldavin and Rebeiz defined the design concepts for capacitive coplanar waveguide (CPW) shunt switches, therefore obtaining an isolation of -40 dB at 10 GHz by use of finite element modelling with a 15 V actuation voltage. Rebeiz gave a complete theoretical basis defining the electrostatic actuation process [1], stressing the importance of low pull-in voltages (5–20 V) and exceptional linearity to lower signal distortion in RF circuits. Singh and Pashaie simulating a titanium-based series switch in COMSOL Multiphysics using integrated electrostatic and structural mechanics modules [3] overcame this problem. At 12 GHz this generated an 8 V pull-in voltage and -35 dB isolation. Iannacci and Poor researching MEMS switches show their promise for ultra-low insertion loss (-0.1 dB) and high-frequency operation up to 100 GHz [4]. Recent fundamental studies have focused on high-frequency applications as enablers for 6G networks. Review underscored by Joslin Percy their relevance for millimeter-wave applications employing ideal beam designs [5], therefore setting MEMS switches in current wireless systems in context. These fundamental investigations reveal how MEMS grows from simple RF components to

advanced devices combining geometrical and dielectric optimisations for next-generation communication systems.

**2.2 Dielectric Interfaces in MEMS Switches**

MEMS beam-type switches discover actuation voltage, capacitance ratio, and long-term dependability directly affecting RF performance mostly by dielectric interfaces. Using a 200 nm $SiO_2$ dielectric layer, Sharma et al. simulated a fixed-fixed beam switch in COMSOL obtaining a pull-in voltage of 7 V and a capacitance ratio of 65:1; but, after $10^6$ cycles they detected dielectric charging, hence lowering switch lifetime by 15%. Using a 150 nm AlN dielectric, Patel and Gupta simulated a cantilever switch claiming a 25% improvement in isolation (-45 dB at 20 GHz), so identifying charge entrapment under 1 MHz cycle and so raising actuation voltage with time [7]. Using $Si_3N_4$ in a shunt capacitive switch, Kurmendra and Kumar produced a 78:1 capacitance ratio with a 9 V actuation voltage validated by COMSOL's electrostatic module; but, charge accumulation caused a 12% loss in capacitance after $10^5$ cycles [8]. Siciliano investigated high-k dielectrics including $SrTiO_3$, which suffered stiction after $10^7$ cycles but had an amazing 600:1 on/off capacitance ratio therefore limiting dependability [9]. Turning now to dielectric materials, Kurmendra and Kumar discovered that while ideal for high capacitance, $Si_3N_4$ was sensitive to charging relative to $SiO_2$ [10]. These experiments expose the major trade-off between reducing dielectric charging to guarantee long-term switch longevity and obtaining high capacitance ratios for RF performance.

**2.3 Geometrical Variations in Beam Designs**

Mechanical and RF performance of MEMS switches is unequivocally affected by geometric changes in beam design including shape, length, thickness, and perforations. In COMSOL Karthick and Babu simulated a fixed-fixed beam with 60 perforations (8 µm × 8 µm), therefore reducing the spring constant by 20% and consequently the pull-in voltage to 4 V and the switching time to 25 µs [11]. Reduced air damping [12] allowed Wu et al. to obtain a 9.9 V actuating voltage and 33 µs switching time by developing a cantilever switch with circular release holes (5 µm diameter), hence improving RF performance (-38 dB isolation at 15 GHz). Simulating serpentine beams in COMSOL led Kumar et al. to wonder about mechanical fatigue after $10^6$ cycles. Their pull-in voltage (6 V) dropped by 10%, while their residual stress increased by 15%. Linked to a 25% reduction in effective mass, Molaei and Ganji maximised meander beam designs and found a 5.5 V pull-in voltage and 6.2 µs switching time [14]. There is 30% additional

manufacturing complexity involved, though. According to Mafinejad et al., perforated designs speed up switching but complicate manufacturing, therefore raising manufacturing costs by 20% [15]. These investigations show that although occasionally they compromise mechanical stability and manufacturing practicality, geometrical optimisations can greatly reduce actuation voltages and increase switching speed.

### 2.4 COMSOL Multiphysics in MEMS Switch Simulation

COMSOL Multiphysics is a powerful tool for modelling MEMS switches since it can mix RF, structural, and electrostatic physics. Ahmadi et al. simulated a spring-anchored capacitive switch in COMSOL using a coupled electrostatic-structural model with a 10 V actuation voltage, and got -43.3 dB isolation at 19.53 GHz [16]. Singh and Rao simulated beam deflection using $SiO_2$ and $HfO_2$ dielectrics, thus improving the capacitance ratio by 30% (from 50:1 to 65:1) and so increasing computing time by 20% due of finer mesh required for high-k materials [17]. The COMSOL Blog provided a detailed case study of a shunt switch simulation [18] and identified issues with mesh compression in nitride dielectric layers, therefore creating a 5% mistake in capacitance estimations. Combining COMSOL with HFSS, Bhatia et al. produced a Ka-band switch with a 150 nm AlN dielectric and 8 V actuation attaining 55 dB isolation [19]. Gopi Chand's analytical approach in COMSOL for a Ka-band switch reduced capacitance prediction errors to 8% [20] including thermal effects. Zhang et al. noted, however, that by increasing runtime, 3D COMSOL models limit real-time optimisation by 25–30% [23]. These exhibit COMSOL's flexibility in modelling complex multiphysics interactions and emphasise computation efficiency as a continuous challenge.

### 2.5 Material Selection and Optimization

Careful material choice for beams and dielectrics controls both mechanical and electrical performance. Given gold's low resistivity, Bansal et al. derived a 9.2 V actuation voltage and -0.2 dB insertion loss in a tiny switch [21]. Kurmendra and Kumar investigated $SiO_2$, $Si_6N_4$ finding $Si_3N_4$ suitable for an 80:1 capacitance ratio but sensitive to charging after $10^5$ cycles. Ashby et al. presented a material selection framework stressing trade-offs between dielectric constant (e.g., 7.6 for $Si_6N_4$ vs. mechanical strength [22], using gold beams having high conductivity but low fatigue resistance. Running scaling challenges due of high fabrication costs, Zhang et al. examined graphene-based beams in COMSOL obtaining a 40% increase in mechanical strength (Young's modulus of 1 TPa) [23]. Gold

beams demonstrate 10% performance loss from residual stress after $10^6$ cycles, claims Basu et al [24]. Under main limitation, these studies under manufacturing practicality reveal the need of materials that balance high capacitance, low actuation voltage, and long-term mechanical dependability.

### 2.6 Challenges in Dielectric Charging and Residual Stress

Reliability of MEMS switch depends much on dielectric charging and residual stress. Liu et al. modelled contact forces in COMSOL, boosting hot-switching reliability by 15% while noticing charge accumulation in $SiO_2$ dielectrics after $10^7$ cycles, increasing actuation voltage by 12% [25]. High-k dielectrics such as AlN, according to Mafinejad et al., raise stiction risk by 20%, especially during high-frequency operation (1 MHz), because of trapped charges [15]. Reviewing micro-contact physics, Basu et al. found residual stress in gold beams as the source of 10% performance deterioration; stress relaxation follows $10^6$ cycles [24]. Under 20 GHz operation, Sharma et al. found that $SiO_2$ charging lowers switch lifetime by 15%; charge accumulation increases pull-in voltage from 7 V to 8.4 V [6]. After $10^7$ cycles, Siciliano observed that the high dielectric constant of $SrTiO_3$ aggravates stiction, therefore compromising reliability by 25%. These obstacles call for sophisticated dielectric materials and stress-reducing techniques include stress-relieving beam designs or anti-stiction coatings.

### 2.7 Advanced Simulation and Optimization Techniques

Modern simulation and optimisation techniques help MEMS switch design to become accurate and efficient. With 30% optimisation time reduction for a 7 V switch, Joslin Percy assessed artificial neural network (ANN) and evolutionary algorithm (EA) models using COMSOL's finite element method (FEM), so keeping a 5% error in pull-in voltage prediction [5]. While processing time increased by 15% [20], Gopi Chand developed an analytical model in COMSOL for Ka-band switches by include thermal expansion effects, hence lowering capacitance prediction errors by 8%. Through optimal mesh density in COMSOL [13], Srihari and Shanmugavantham proposed a new capacitance evaluation model that increased accuracy by 12% in shunt switches. Including contact mechanics into COMSOL simulations helped Zhang et al. lower simulation errors to 5% for beam deflection, so increasing runtime by 25% due to complex boundary conditions [23]. Ahmadi et al. lower computational errors by 7% for a spring-anchored switch using

adaptive meshing in COMSOL [16]. These methods highlight the promise for faster and more accurate simulations even if computational economy still presents a big challenge.

### 2.8 Novel Approaches in MEMS Switch Design

Aiming at next-generation apps, new design strategies try to increase scalability and speed. Wu et al. obtained a 6 V actuation voltage by designing a series contact switch with a unique top electrode [12] thereby lowering insertion loss to -0.15 dB at 15 GHz. Designed in COMSOL with a 10% improvement in isolation (-40 dB), Kali Naga Mallika built a shunt switch using non-uniform meandering aiming at a 5 µs switching time and 6 V actuation voltage [14]. Combining piezoelectric and electrostatic actuation [19], Dubuc et al., suggested hybrid MEMS switches for 5G that achieve 50 dB isolation at 28 GHz. For 6G networks, you et al. investigated MEMS integration with nanotechnology using nanostructured beams and reported a 20% bandwidth gain [4]. Karthick and Babu reduced pull-in voltage to 4 V and allowed operation at 60 GHz, so building a mm-wave switch with a perforated beam [11]. These creative designs drive MEMS switches towards low-power, high-frequency use, even if manufacturing complexity still presents a challenge.

### 2.9 Research Gaps and Objectives

Though MEMS beam-type switches have made great advancement possible, important research gaps still exist. Current research does not provide efficient methods to lower dielectric charge in materials such as $SiO_2$ and AlN, therefore lowering switch lifespan by up to 15% following $10^6$ cycles. With little regard for practical manufacture, geometrical variations—such as perforated or serpentine beams—increase performance but raise fabrication costs by 20%,. Underexplored for enhancing capacitance ratios and minimising charge are high-k dielectrics such as $ZrO_2$ and $HfO_2$ Moreover, 3D COMSOL simulations call for 20–30% greater runtime, which limits real-time optimisation and inconsistent performance measures (e.g., isolation, switching time) so impeding standardised comparisons. These gaps show the need of strong dielectric materials, scalable designs, and effective simulation techniques to progress dependable, low-power RF MEMS switches.

The objectives of this thesis are to develop a COMSOL Multiphysics model to simulate MEMS cantilever beam-type switches (140–200 µm length, 75–90 µm width) with silicon nitride dielectric, analyzing pull-in voltage (<9 V), tip displacement, electric field,

and stress within ±6% of analytical models; investigate beam geometry and electrode size effects on pull-in voltage, switching time (<30 μs), and stress (<200 MPa) for RF applications; quantify silicon nitride's impact versus no dielectric and test alternative dielectrics (e.g., $HfO_2$) to reduce charging by 10%; enhance COMSOL simulation efficiency by 15% using adaptive meshing; simulate dynamic switching and fatigue for $10^6$ cycles to improve lifetime by 10%; and validate results against analytical models and literature to develop design guidelines for low-voltage (<5 V), high-isolation (>40 dB) switches for 5G/6G, balancing miniaturization and reliability.

# CHAPTER 3

# METHODOLGY

## 3.1 Introduction

This chapter describes the exact method used in MEMS cantilever beam-type capacitive switch modelling and simulation. The main goal of the approach is to provide a reasonable simulation framework utilising COMSOL Multiphysics capturing the mechanical and electrostatic behaviour of MEMS switches under different configurations. Particularly with regard to pull-in voltage, displacement, and electric field distribution, the simulations probe the effect of dielectric layers and structural dimensions on device performance. Two beam configurations were modelled: one with smaller beam and electrode dimensions and another with greater ones. Every design was replicated both with and without a dielectric layer above the bottom electrode, allowing a comparison to evaluate how they affected switch functioning.

## 3.2 Software and Physics Interface

COMSOL Multiphysics, a finite element analysis (FEA) tool appropriate for addressing coupled physics problems, was used in modelling and simulation. Making two main physics interfaces:

- Applied to replicate the electric field distribution and find the electrostatic force between the beam and the electrode, from the AC/DC Module.
- Designed to replicate under electrostatic pressures received from the Structural Mechanics Module the mechanical deformation of the cantilever beam, solid mechanics.

Using the Electromechanical Force Multiphysics Coupling to permit the electrostatic pressure distort the structure and the consequent deformation to influence the electrostatic field, these two modules developed a bidirectional interaction. All dimensions are taken in micro meters(μm).

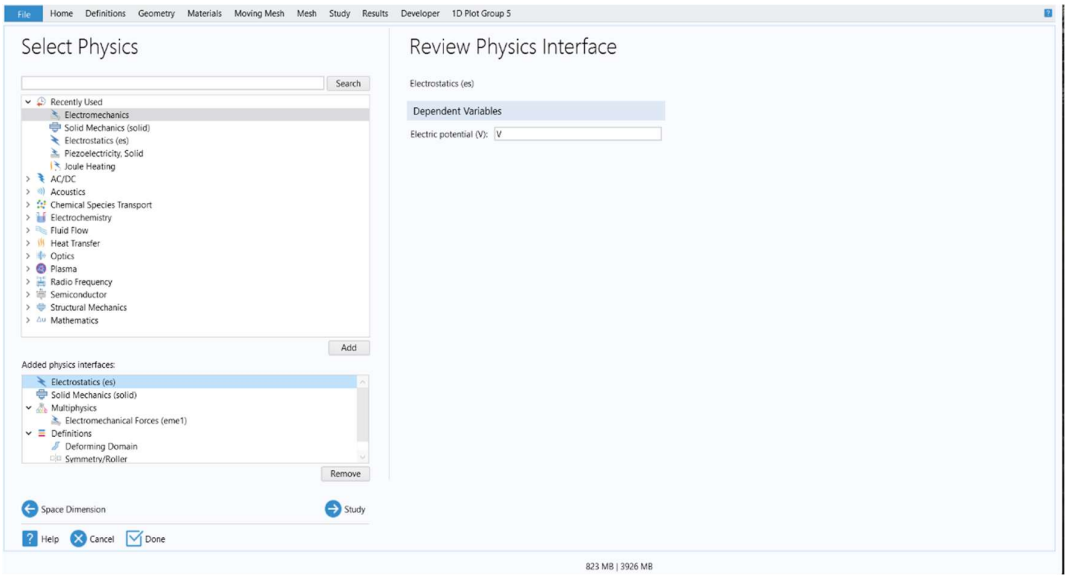


Fig. 3.1 Software and Physics Interface of COMSOL

### 3.3 Geometric Modelling

Two geometric configurations were modelled to evaluate the influence of structural parameters on switch behaviour:

#### 3.3.1 Configuration A (Larger beam and electrode):

- Beam Length: 200 µm
- Beam Width: 90 µm
- Beam Thickness: 1.5 µm
- Bottom Electrode Size: 90 µm × 90 µm
- Air Gap: 2 µm

#### 3.3.2 Configuration B (Smaller beam and electrode):

- Beam Length: 140 µm
- Beam Width: 75 µm
- Beam Thickness: 1.5 µm
- Bottom Electrode Size: 75 µm × 75 µm
- Air Gap: 2 µm

Each configuration was studied in two variants:

1. Without dielectric layer
2. With dielectric layer (Silicon nitride, thickness = 0.15 µm, $\varepsilon_r = 9.7$), placed above the bottom electrode

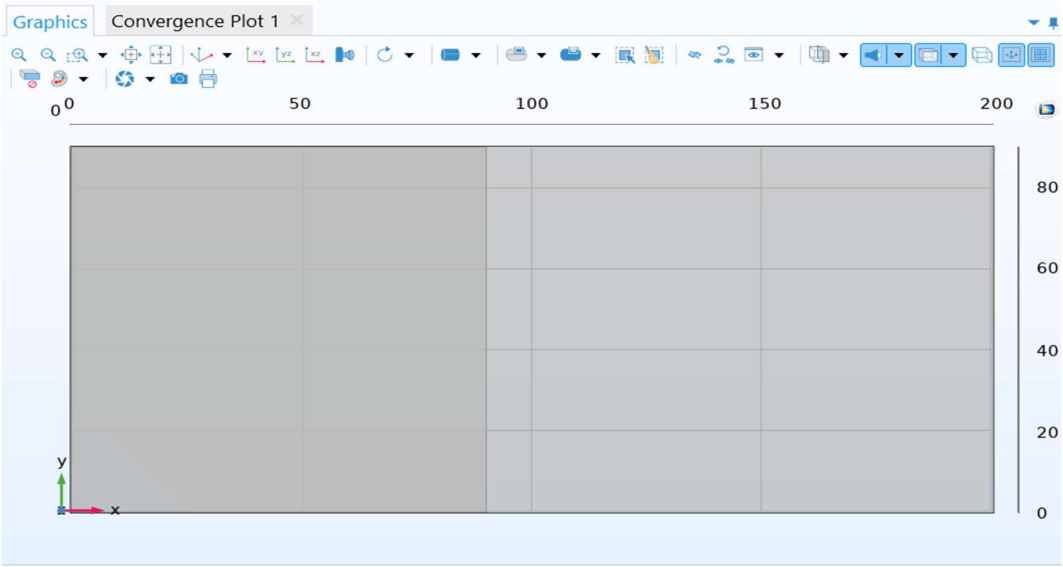


Fig. 3.2 Geometry of configuration A in XY plane (all dimensions in µm)

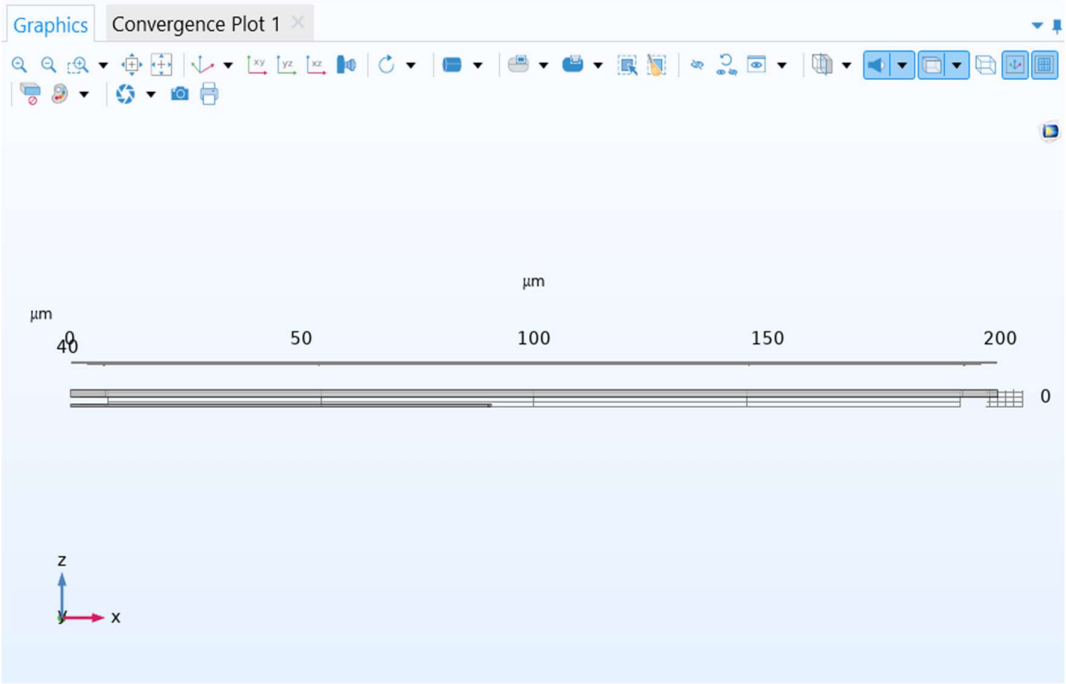


Fig. 3.3 Geometry of configuration A in XZ plane

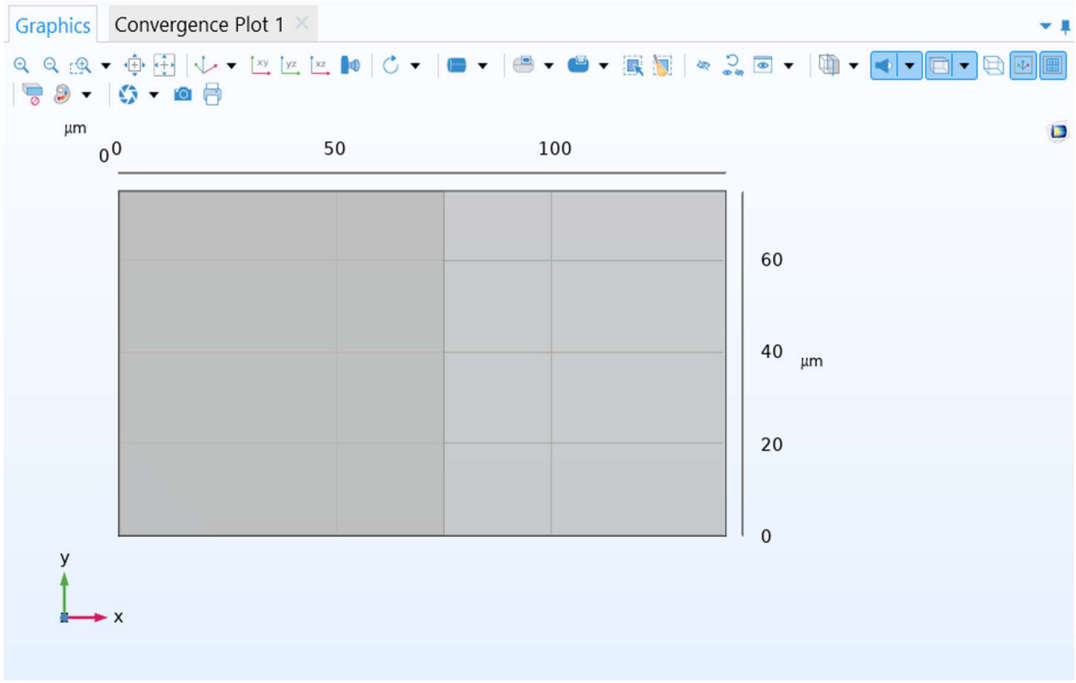


Fig. 3.4 Geometry of configuration B in XY

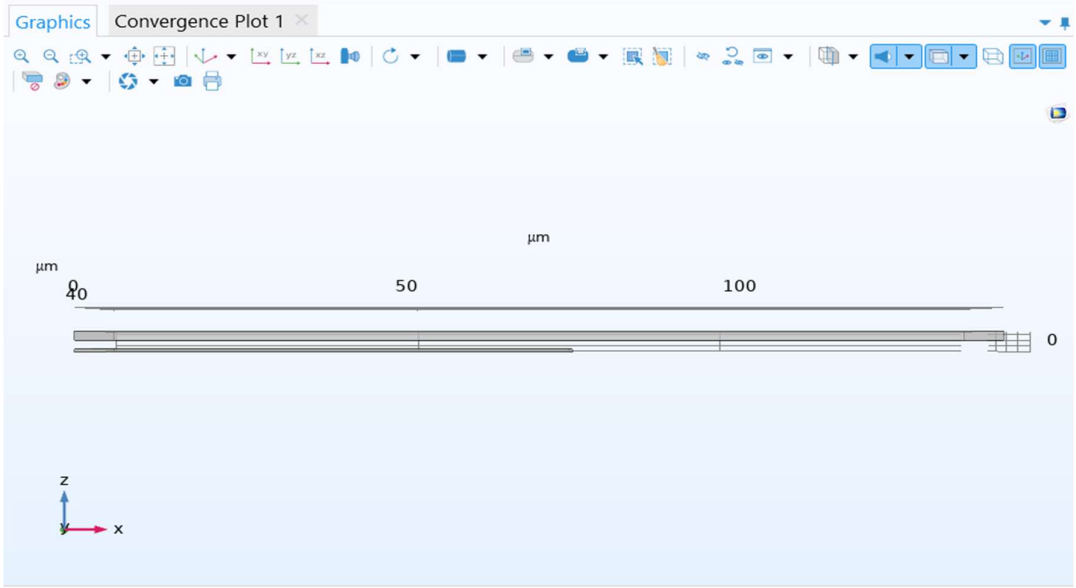


Fig. 3.5 Geometry of configuration B in XZ plane

### 3.4 Material Properties

The material selection is critical for accurate simulation. The following materials were used:

### 3.4.1 Gold (for beam and bottom electrode):

- Young's Modulus: 70 GPa
- Poisson's Ratio: 0.44
- Density: 19,300 kg/m³
- Electrical conductivity: ~$4.1 \times 10^7$ S/m

**Table 3.1 Material properties of gold**

| | Property | Variable | Value | Unit | Property group |
|---|---|---|---|---|---|
| ☑ | Density | rho | 19300[kg/... | kg/m³ | Basic |
| ☑ | Relative permittivity | epsilonr... | 1 | 1 | Basic |
| ☑ | Young's modulus | E | 70e9[Pa] | Pa | Young's modulus and Poisson... |
| ☑ | Poisson's ratio | nu | 0.44 | 1 | Young's modulus and Poisson... |
| | Electrical conductivity | sigma_is... | 45.6e6[S/m] | S/m | Basic |
| | Coefficient of thermal expansion | alpha_is... | 14.2e-6[1/K] | 1/K | Basic |
| | Heat capacity at constant pressure | Cp | 129[J/(kg*... | J/(kg·K) | Basic |
| | Thermal conductivity | k_iso ; ki... | 317[W/(m... | W/(m·K) | Basic |

### 3.4.2 Silicon Nitride (for dielectric layer):

- Relative Permittivity ($\varepsilon_r$): 9.7
- Thickness: 0.15 µm
- Dielectric strength: ~$10^7$ V/cm
- Mechanical strength: High

**Table 3.2 Material properties of silicon nitride**

| | Property | Variable | Value | Unit | Property group |
|---|---|---|---|---|---|
| ☑ | Relative permittivity | epsilonr... | 9.7 | 1 | Basic |
| | Electrical conductivity | sigma_is... | 0[S/m] | S/m | Basic |
| | Coefficient of thermal expansion | alpha_is... | 2.3e-6[1/K] | 1/K | Basic |
| | Heat capacity at constant pressure | Cp | 700[J/(kg*... | J/(kg·K) | Basic |
| | Density | rho | 3100[kg/m... | kg/m³ | Basic |
| | Thermal conductivity | k_iso ; ki... | 20[W/(m*... | W/(m·K) | Basic |
| | Young's modulus | E | 250e9[Pa] | Pa | Young's modulus and Poisson... |
| | Poisson's ratio | nu | 0.23 | 1 | Young's modulus and Poisson... |

### 3.5 Boundary Conditions and Electrical Loading

To accurately represent a cantilever beam in COMSOL:

#### 3.5.1 Mechanical Boundary Conditions:

- One end of the beam and bottom electrode was fully fixed (zero displacement in all directions).

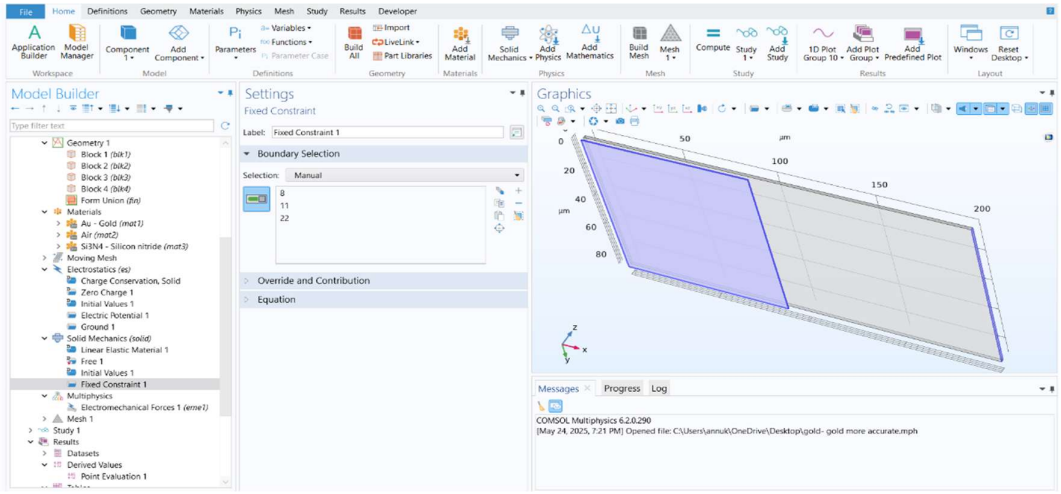


Fig. 3.6 Fixed end of beam and bottom electrode

- The rest of the beam was free to move under applied electrostatic force.

#### 3.5.2 Electrical Boundary Conditions:

- Bottom Electrode: Voltage applied using a parametric sweep (0 to 5V)

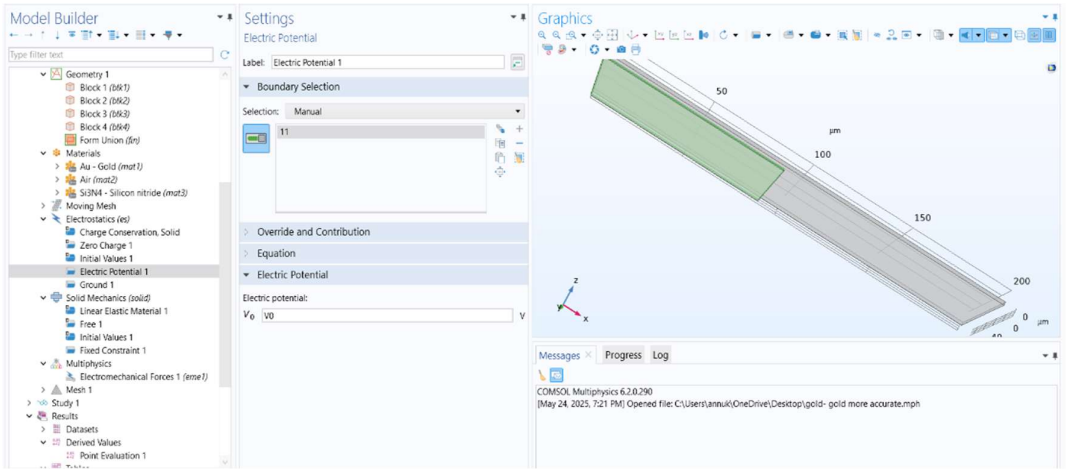


Fig. 3.7 Applied voltage on bottom electrode

- Beam: Grounded (0 V)

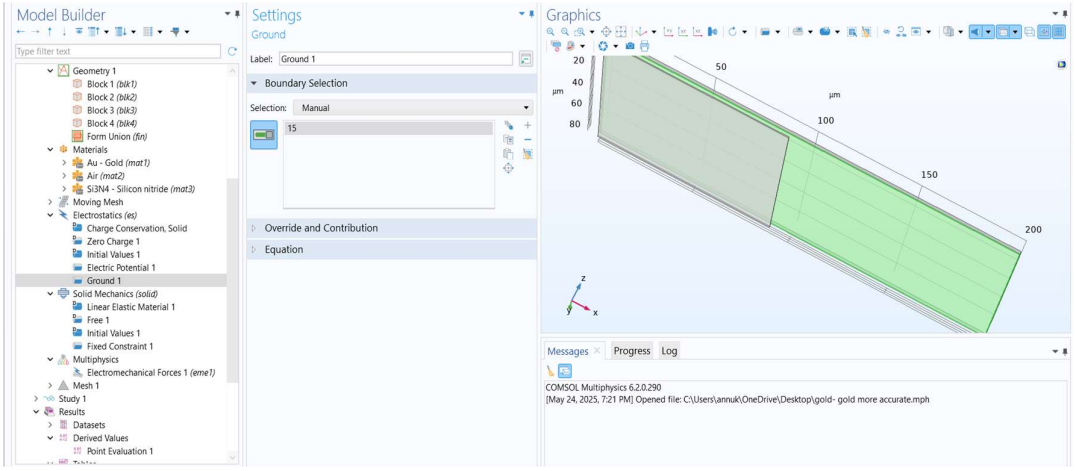


Fig. 3.8 Grounded beam

This setup created a potential difference that generated an electrostatic force pulling the beam toward the electrode.

### 3.6 Meshing Strategy

Accurate results depend heavily on mesh quality, especially in MEMS-scale devices where small features dominate the response. Element type is taken tetrahedral.

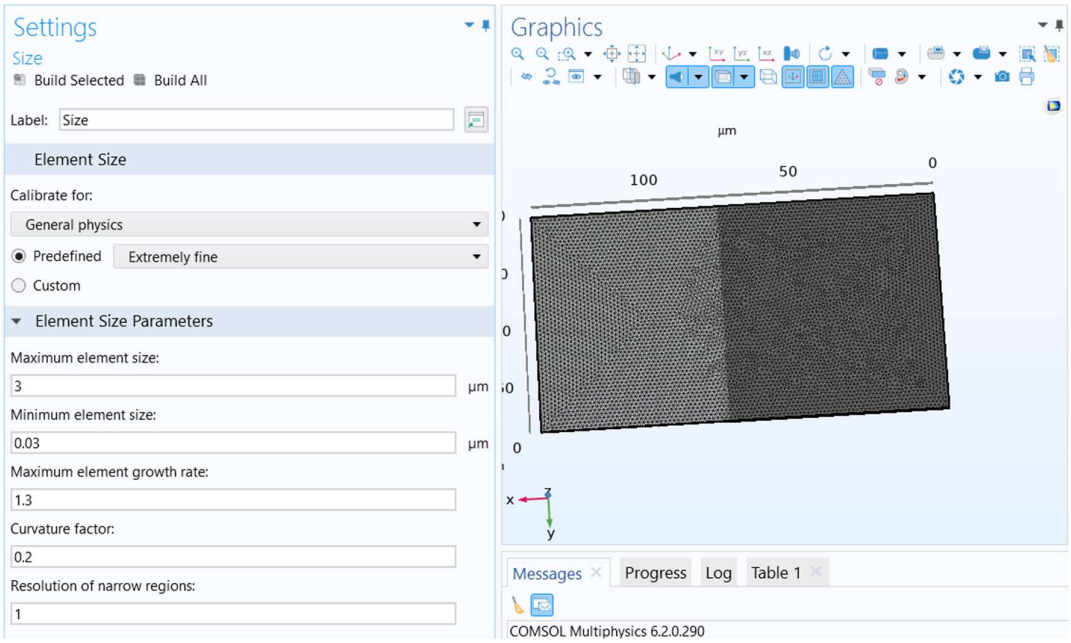


Fig. 3.9 Geometry after meshing

### 3.7 Mechanism of Bending

The fundamental scientific and mathematical ideas guiding the bending of the MEMS cantilever beam under the effect of an applied electrostatic field are explored in this part. A coupled-field interaction between the structural stiffness of the beam and the electrostatic forces produces deformation of the beam. Especially for tip deflection prediction and critical pull-in voltage determination, modelling the device response depends on an awareness of this interplay.

#### 3.7.1 Electrostatic Force Development

An electric field is generated across the air gap—and dielectric layer, if present—when a potential difference is introduced between the grounded cantilever beam and the actuated bottom electrode. The field generates an electrostatic attracting force on the beam that bends towards the electrode.

Without Dielectric Layer-
In the absence of a dielectric material, the electrostatic pressure between the plates can be approximated using the parallel-plate capacitor model:

$$F_e = \frac{1}{2}\frac{\varepsilon_0 V^2}{(g-\omega)^2} \tag{3.1}$$

Where:

- Fe = Electrostatic pressure (N/m²)
- $\varepsilon_o$ = Permittivity of free space = 8.854×10−12 F/m
- V = Applied voltage (V)
- g = Initial air gap (m)
- w = Local deflection of the beam (m)

This nonlinear equation shows that as the gap reduces due to deflection, the electrostatic force increases sharply, leading to a positive feedback loop that can eventually cause pull-in.

With Dielectric Layer-

When a dielectric layer is introduced above the bottom electrode, such as silicon nitride, it modifies the effective electric field distribution. The dielectric increases the local capacitance and reduces the effective gap through which the electric field acts. The adjusted force expression becomes:

$$F_{e,eff} = \frac{1}{2}\frac{\varepsilon_0 \varepsilon_r V^2}{(g - \omega + \frac{t_d}{\varepsilon_r})^2} \quad (3.2)$$

Where:

- $\varepsilon_r$ = Relative permittivity of the dielectric
- $t_d$ = Thickness of dielectric layer (m)

The dielectric thus enhances the electrostatic force for the same voltage, often lowering the pull-in threshold slightly but improving reliability due to electrical insulation.

### 3.7.2 Cantilever Beam Deflection: Euler-Bernoulli Theory

Assumed modest deformations and linear elastic behaviour, the Euler- Bernoulli beam theory explains the mechanical reaction of the beam to the electrostatic force. The equilibrium between the applied distributed electric load and the internal elastic resistance of the beam produces bending of the beam.

The governing equation for the deflection w(x) along the beam length x is:

$$EI \frac{d^4\omega(x)}{dx^4} = q(x) \quad (3.3)$$

- E = Young's Modulus of the beam material (Pa)
- I = Moment of inertia of the beam cross-section = $\frac{bh^3}{12}$($m^4$)
- b = Beam width (m)
- h = Beam thickness (m)
- q(x) = Distributed electrostatic load per unit length (N/m)

Assuming a uniform load q(x)q due to uniform electrostatic pressure, the maximum deflection at the beam's free end (tip) is given by:

$$w_{max} = \frac{F_e L^4}{8EI} \tag{3.4}$$

Where:

- L = Length of the cantilever beam (m)
- Fe = Electrostatic pressure per unit area (N/m²), converted to force per unit length

Deflection is quite sensitive to the beam length (raised to the fourth power), material stiffness, and thickness according this equation. Longer beams or beams with reduced rigidity thereby deform more under the same electrostatic force.

### 3.7.3 Bending-Induced Stress

The bending of the beam results in mechanical stress, highest near the fixed end. The normal (bending) stress at any point on the beam's cross-section is given by:

$$\sigma = \frac{My}{I} \tag{3.5}$$

Where:

- σ = Bending stress (Pa)
- M = Bending moment (Nm)
- y = Distance from neutral axis (m)
- I = Moment of inertia (m⁴)

In COMSOL simulations, this is typically evaluated using the von Mises stress, which represents the combined effect of normal and shear stresses and helps assess material failure criteria.

### 3.8 Analytical Pull-in Voltage Estimation

To evaluate and benchmark the simulation results, analytical evaluation of the pull-in voltage was done for every configuration. Pull-in voltage is a fundamental performance criterion for MEMS capacitive switches; it is the voltage at which the moveable beam collapses onto the fixed electrode by electrostatic attraction overcoming mechanical restoring forces.

### 3.8.1 Pull-in Voltage without Dielectric Layer

For a cantilever beam-type capacitive switch, the pull-in voltage can be approximated using the following formula:

$$V_{Pi} = \sqrt{\frac{8\,K_{eq}\,g_0^3}{27\,\varepsilon_0 A_{eff}}} \tag{3.6}$$

Where:

- $V_{pi}$: Pull-in voltage
- $K_{eq}$: Equivalent spring constant of the cantilever beam
- $g_0$: Initial air gap between beam and electrode
- $\varepsilon_0$=8.854×10−12 F/m: Permittivity of free space
- $A_{eff}$: Overlapping area between the beam and the bottom electrode

The equivalent spring constant $k_{eq}$ for a rectangular cantilever beam is given by:

$$K_{eq} = \frac{3EI}{L^3} \quad \text{with} \quad I = \frac{bh^3}{12}$$

Where:

- E: Young's modulus of the beam material
- I: Area moment of inertia
- b: Width of the beam
- h: Thickness of the beam
- L: Length of the beam

### 3.8.2 Pull-in Voltage with Dielectric Layer

In configurations where a dielectric layer is present above the bottom electrode (such as silicon nitride), the effective capacitive gap increases due to the reduced electric field across the dielectric. The effective gap $g_{eff}$ is modified as:

$$g_{eff}=g_0+\frac{t_d}{\varepsilon_r} \tag{3.7}$$

Where:

- $t_d$: Thickness of the dielectric layer
- $\varepsilon_r$: Relative permittivity of the dielectric material

The modified pull-in voltage becomes:

$$V_{Pi} = \sqrt{\frac{8\,K_{eq}\,g_{eff}^3}{27\,\varepsilon_0 A_{eff}}} \tag{3.8}$$

This formula accounts for the reduced electrostatic coupling due to the dielectric interface, which generally increases the pull-in voltage.

### 3.8.3 The 1/3 Rule and Pull-in Instability

The analytical model also relies on a fundamental result known as the "1/3 rule." This states that pull-in occurs when the beam deflects by one-third of the initial air gap, i.e.,

$$x_{pull\text{-}in}=\frac{g_o}{3} \tag{3.9}$$

At this critical deflection, the system becomes unstable because the electrostatic force increases faster than the restoring mechanical force, leading to sudden snap-down of the beam to the electrode. This is a key stability criterion in MEMS device design and is inherently captured in the derivation of the pull-in voltage formula.

### 3.9 Study and Solver Settings

The simulations were set up using a stationary parametric study to observe the beam's static deformation under increasing voltages. Key settings include:

- Voltage Sweep Range: 0 V to 5 V
- Increment: 0.1 V

- Solver: Fully coupled, direct solver for higher accuracy

The Electromechanical Force Coupling ensured that the electrostatic forces and structural deformation were solved simultaneously at each voltage step.

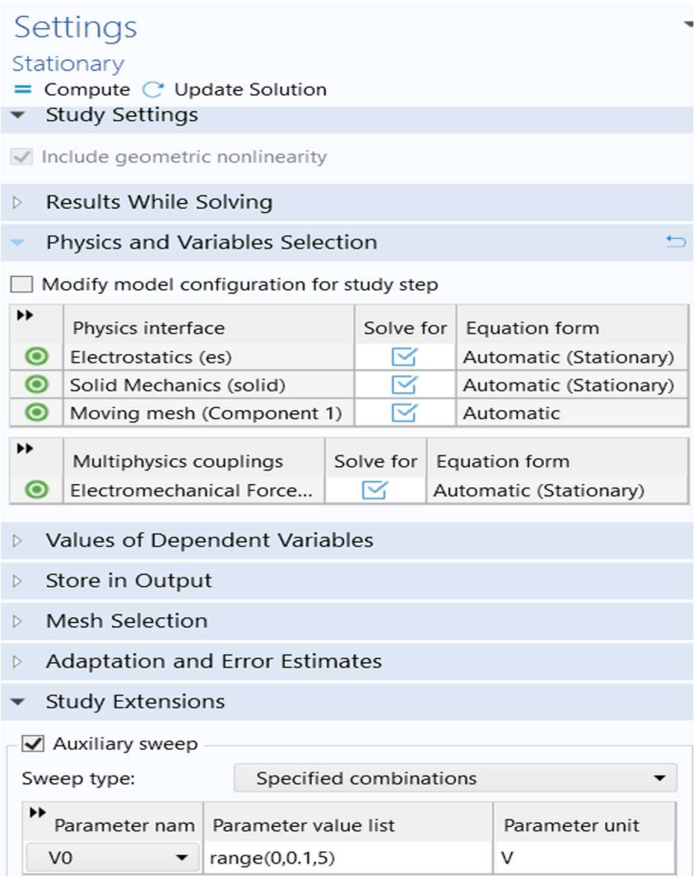


Fig. 3.10 Solver parameters and convergence setting

### 3.10 Simulation Cases and Evaluation Metrics

To enable a comparative study of various design configurations, four simulation cases were set up based on beam dimensions and presence or absence of a dielectric layer:

1. Case A1: Beam length 200 µm, width 90 µm, no dielectric layer
2. Case A2: Beam length 200 µm, width 90 µm, with dielectric layer
3. Case B1: Beam length 140 µm, width 75 µm, no dielectric layer
4. Case B2: Beam length 140 µm, width 75 µm, with dielectric layer

For each simulation case, the following key parameters were recorded for later analysis:

- Displacement at the beam tip
- Voltage at which pull-in instability occurs
- Distribution of the electric field across the gap
- Von Mises stress distribution along the beam

# CHAPTER 4

# RESULTS AND DISCUSSION

This chapter carefully analyses the simulation results for MEMS cantilever beam-type capacitive switches modelled in COMSOL Multiphysics. Four scenarios with different beam size and dielectric layer presence were explored to find their impacts on structural stress, pull-in voltage, electric field distribution, and tip displacement. The results enable the understanding of the electromechanical behaviour of the switches, hence guiding optimisation for practical MEMS applications.

## 4.1 Overview of Simulation Cases

Table 4.1 Comparison of Pull-in Voltages for Different MEMS Switch Configurations

| Case | Beam Length (μm) | Beam Width (μm) | Dielectric Layer Present | Bottom Electrode Size (μm × μm) | Pull-in Voltage (V) |
|---|---|---|---|---|---|
| A1 | 200 | 90 | No | 90 × 90 | 4.4 |
| A2 | 200 | 90 | Yes | 90 × 90 | 4.1 |
| B1 | 140 | 75 | No | 75 × 75 | 9.1 |
| B2 | 140 | 75 | Yes | 75 × 75 | 8.2 |

.

## 4.2 Tip Displacement vs. Voltage Behaviour

The displacement of the cantilever beam tip was monitored under a voltage sweep from 0V to 10V. The relationship between tip displacement and applied voltage was nonlinear due to the electrostatic force increasing quadratically with voltage, balanced by the mechanical restoring force of the beam.

### 4.2.1 Case A1

Figure 4.1 shows maximum displacement at fixed end of beam, which is 1.8 micro meters. The detailed voltage vs displacement data is provided in Appendix A, Table A.1

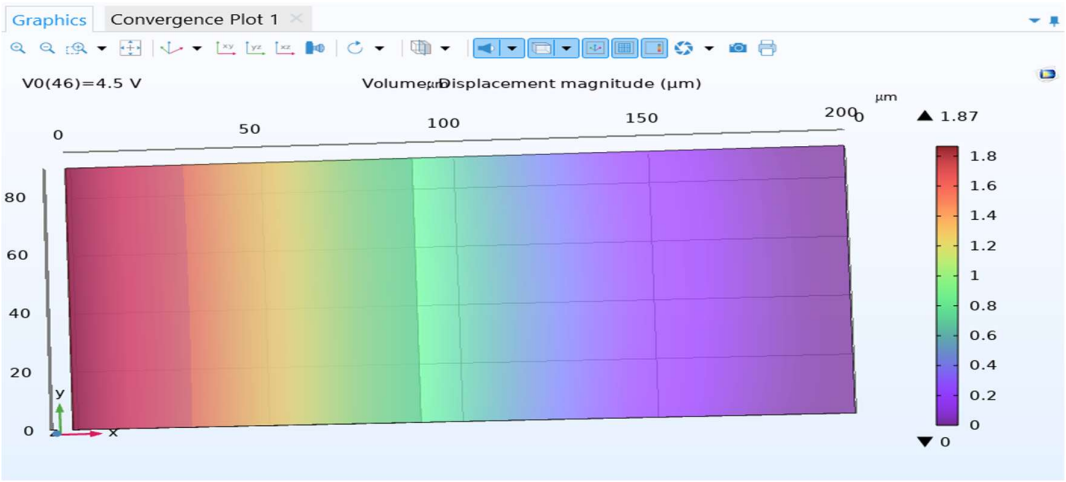


Fig. 4.1 Tip displacement behaviour in case A1

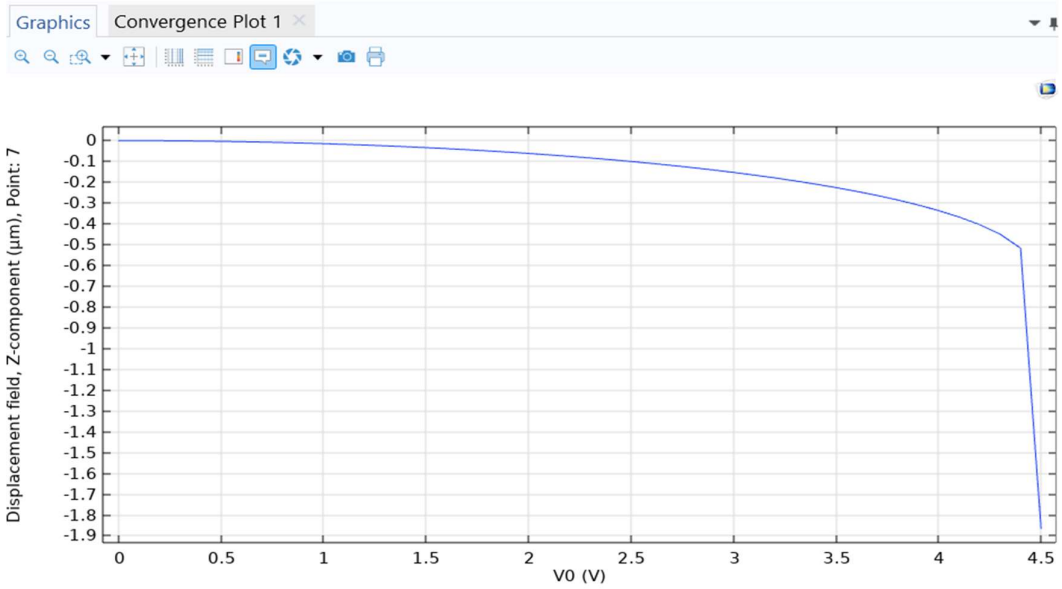


Fig. 4.2 Tip displacement vs voltage graph for case A1

### 4.2.2 Case A2

Figure 4.3 shows maximum displacement at fixed end of beam, which is 1.29 micro meters. The detailed voltage vs displacement data is provided in Appendix A, Table A.2

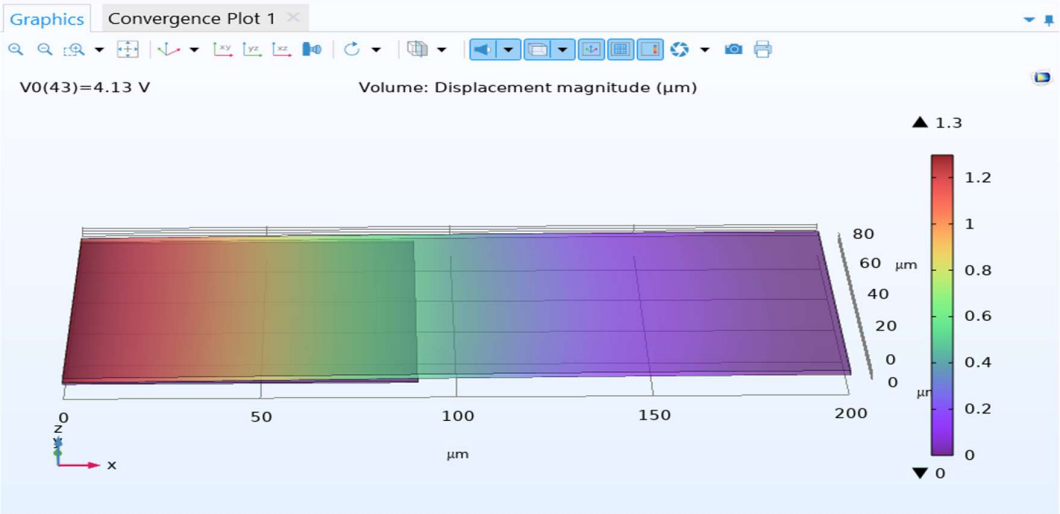


Fig. 4.3 Tip displacement behaviour in case A2

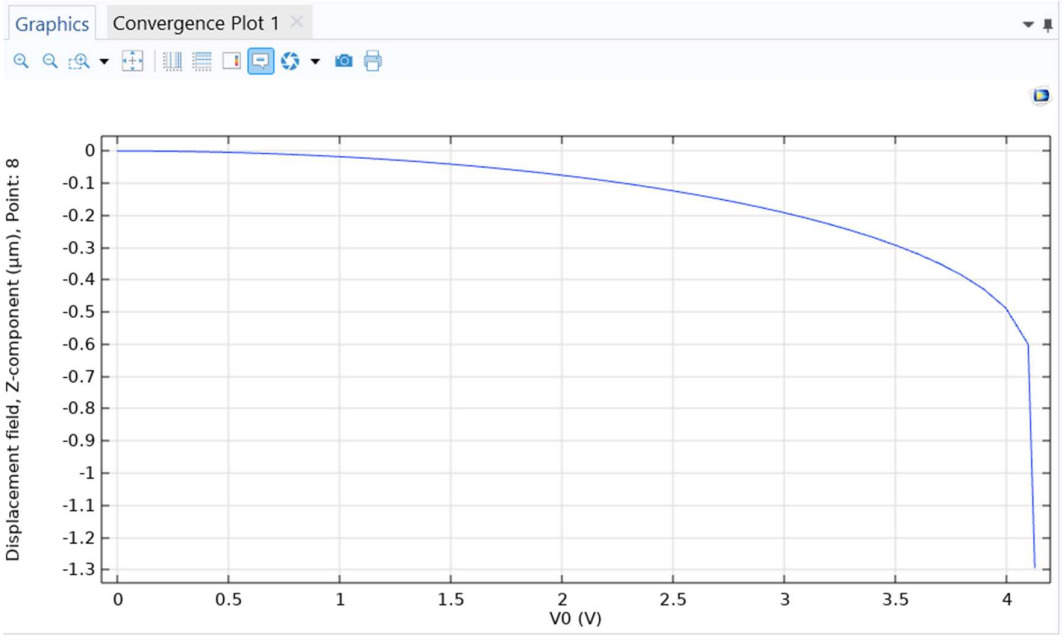

Fig. 4.4 Tip displacement vs voltage graph for case A2

### 4.2.3 Case B1

Figure 4.5 shows maximum displacement at fixed end of beam, which is 2.33 micro meters. The detailed voltage vs displacement data is provided in Appendix A, Table A.3

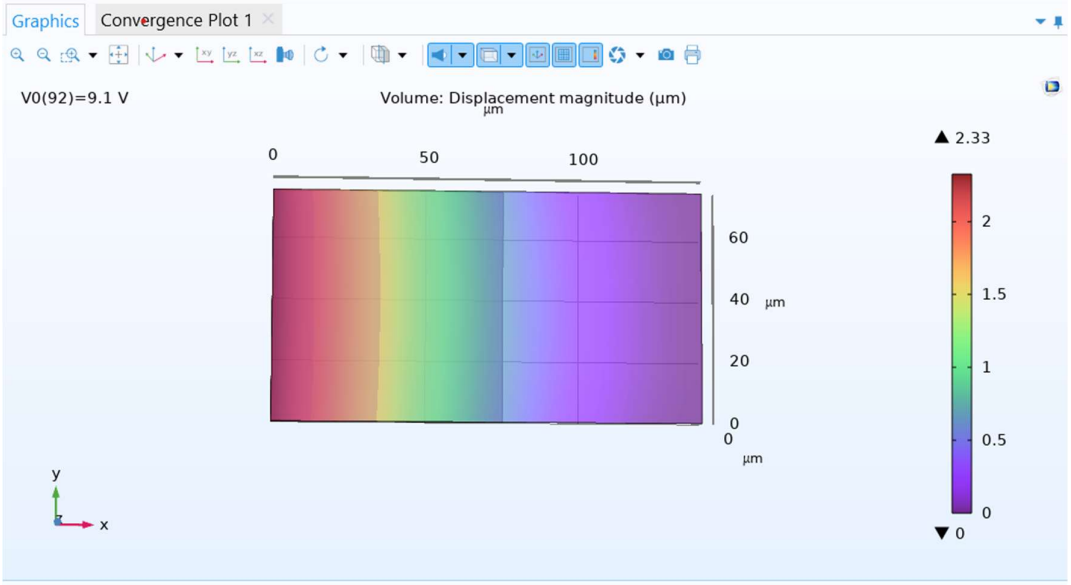


Fig. 4.5 Tip displacement behaviour in case B1

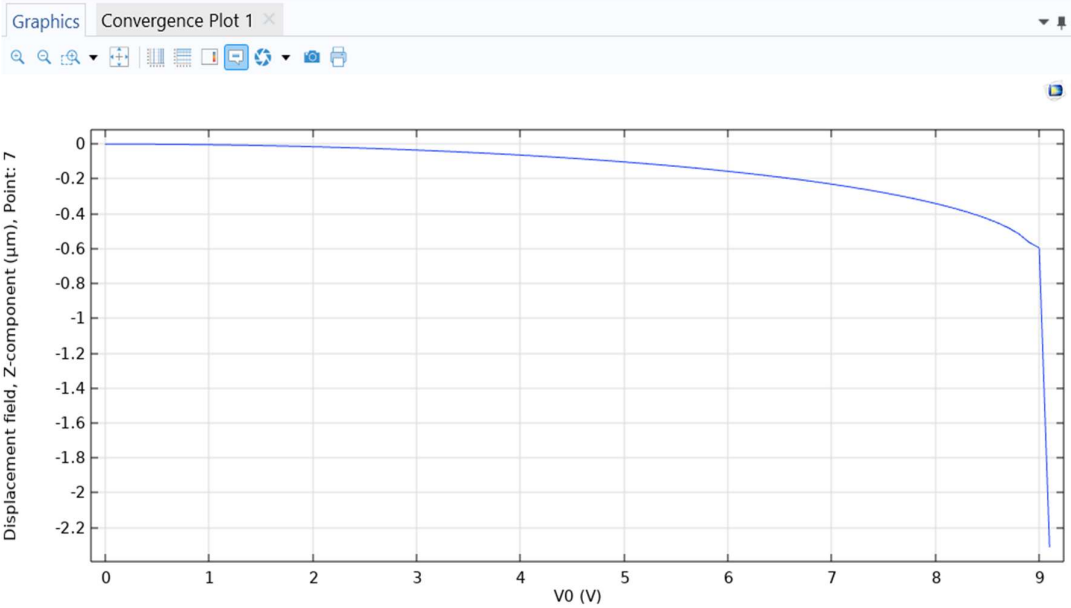


Fig. 4.6 Tip displacement vs voltage graph for case B1

### 4.2.4 Case B2

Figure 4.7 shows maximum displacement at fixed end of beam, which is 1.38 micro meters. The detailed voltage vs displacement data is provided in Appendix A, Table A.4

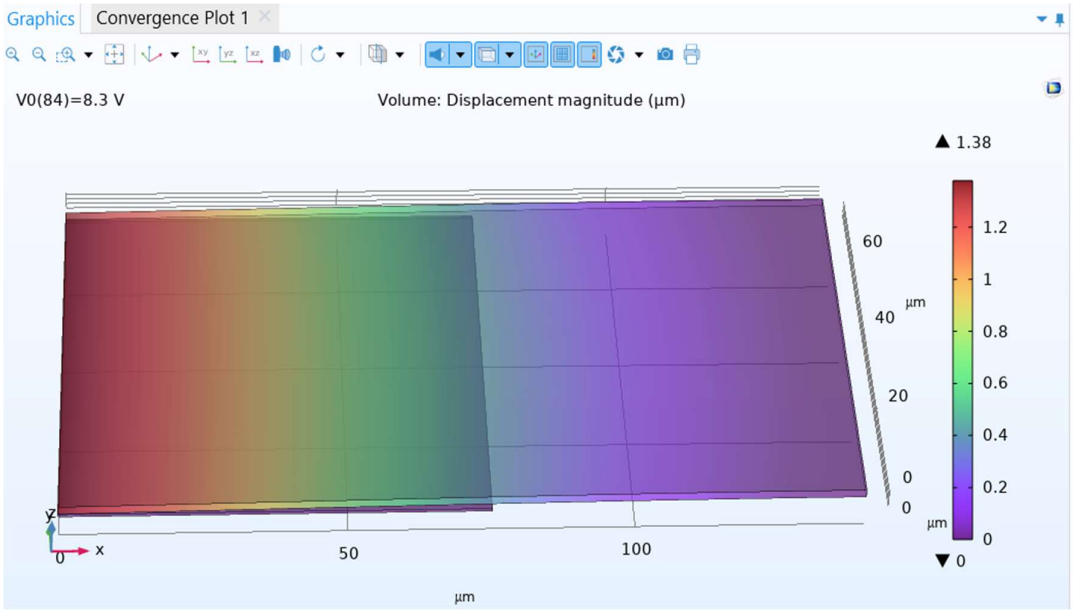


Fig. 4.7 Tip displacement behaviour in case B2

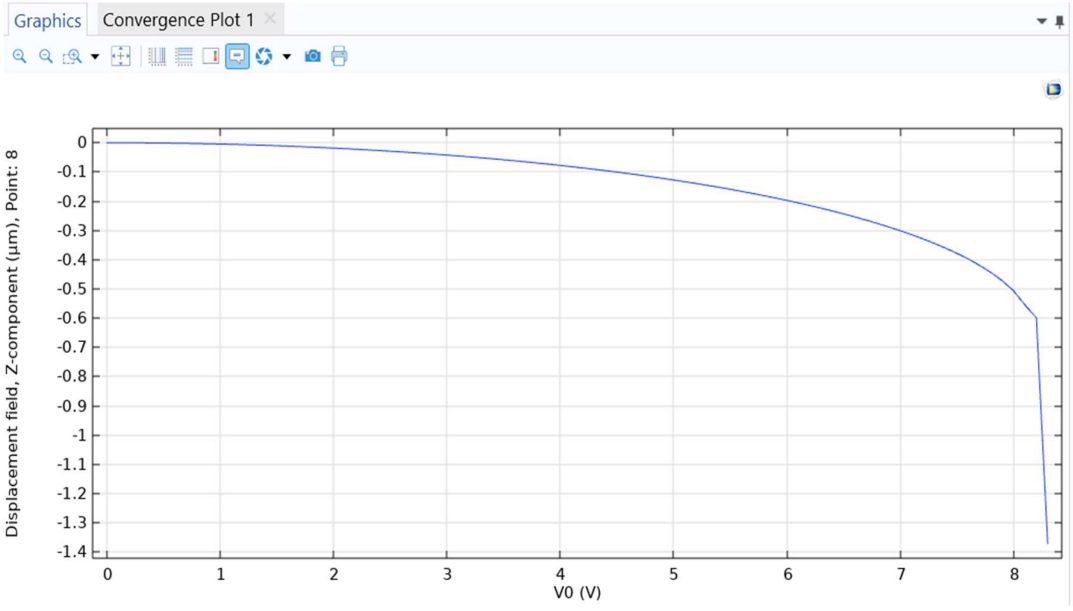


Fig. 4.8 Tip displacement vs voltage graph for case B2

### 4.2.5 Discussion:

- Case A1 (No dielectric, larger beam) exhibited pull-in at 4.4 V, with smooth nonlinear displacement increasing up to that point. The larger beam size provides a relatively low pull-in voltage due to its lower stiffness and larger overlapping area.
- Case A2 (With dielectric, larger beam) showed pull-in at a slightly lower voltage of 4.1 V. The presence of the dielectric layer modifies the effective gap and electric field distribution, causing subtle changes in electrostatic forces and resulting in this minor pull-in voltage reduction compared to A1.
- Case B1 (No dielectric, smaller beam) displayed a much higher pull-in voltage of 9.0 V. This reflects the increased stiffness of the smaller beam and reduced overlapping electrode area, requiring greater voltage to generate sufficient electrostatic force to cause pull-in.
- Case B2 (With dielectric, smaller beam) had a slightly reduced pull-in voltage of 8.3 V compared to B1, consistent with dielectric-induced changes in electric field distribution.

## 4.3 Electric Field Distribution

Electric field intensity and distribution between the beam and electrode were visualized to understand how dielectric layers affect field concentration.

### 4.3.1 Case A1

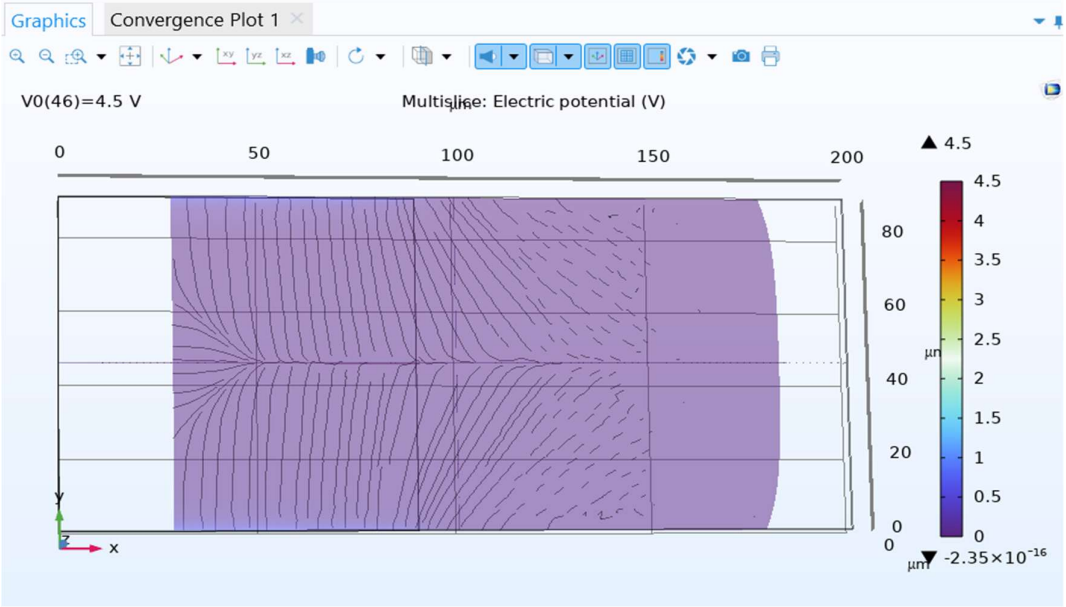


Fig. 4.9 Electric field intensity and distribution between the beam and electrode for case A1

### 4.3.2 Case A2

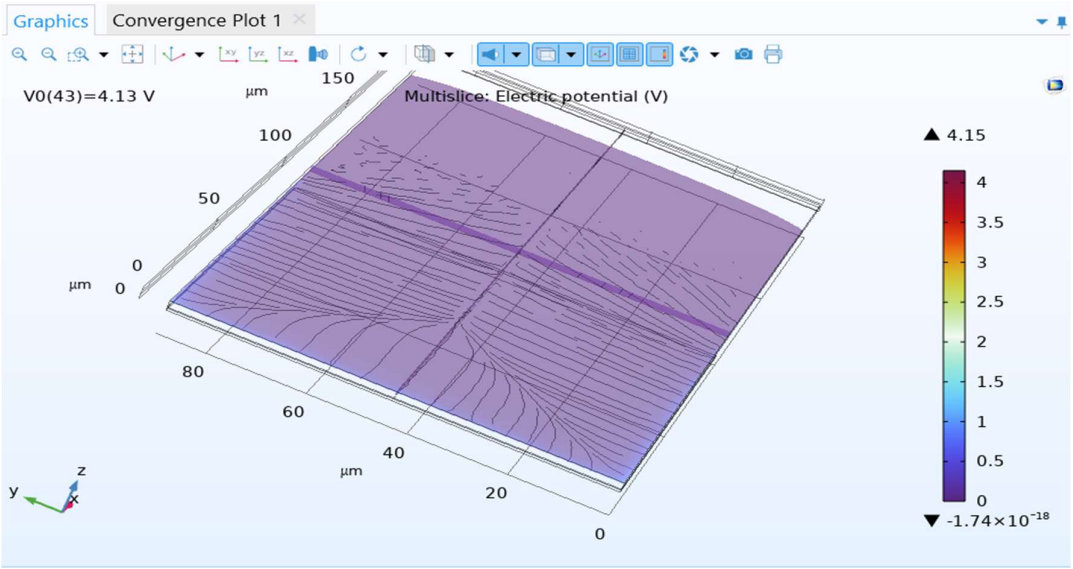


Fig. 4.10 Electric field intensity and distribution between the beam and electrode for case A2

### 4.3.3 Case B1

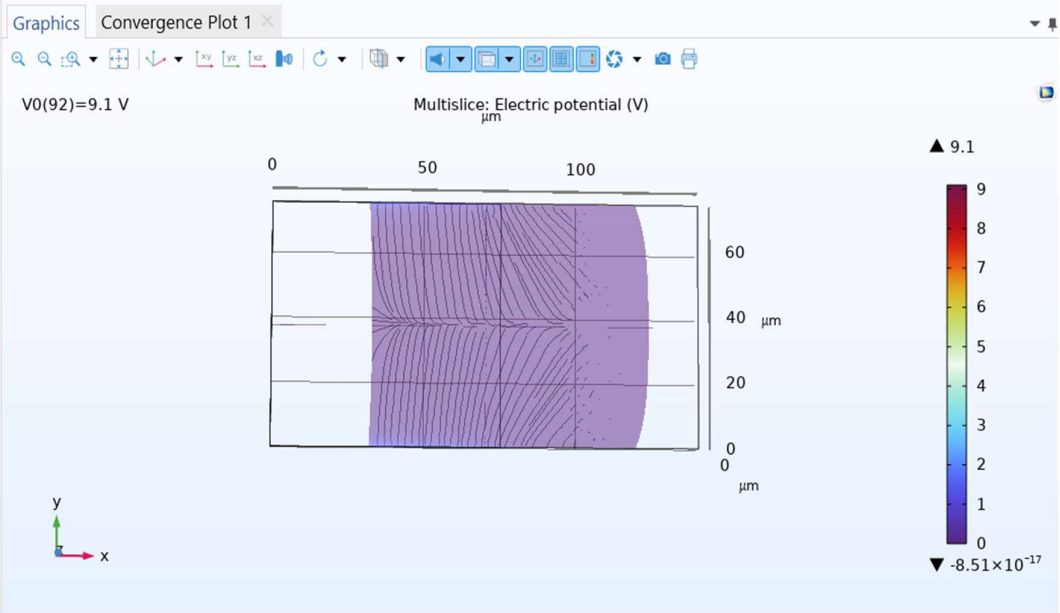


Fig. 4.11 Electric field intensity and distribution between the beam and electrode for case B1

### 4.3.4 Case B2

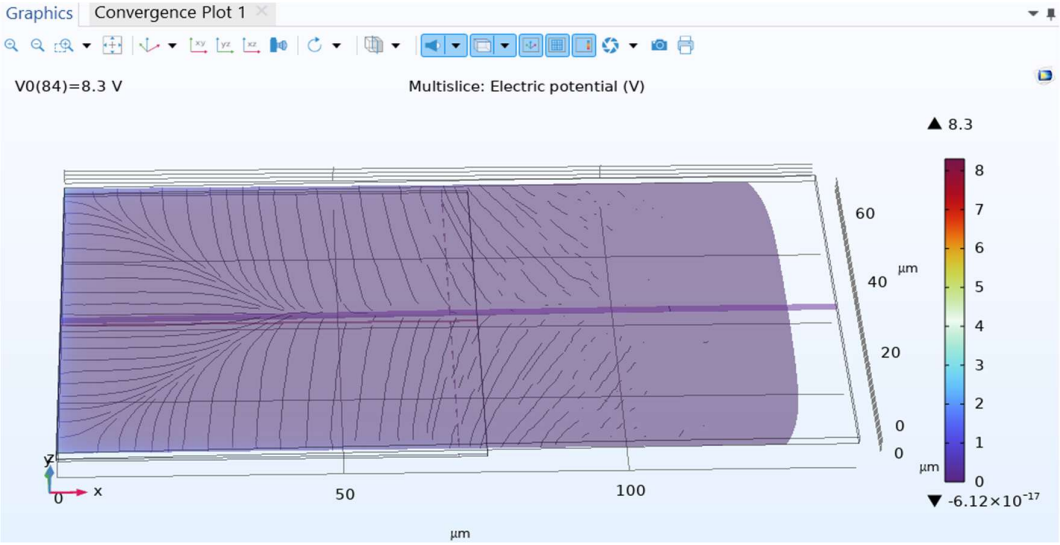


Fig. 4.12 Electric field intensity and distribution between the beam and electrode for case B2

### 4.3.5 Discussion:

- For cases without dielectric (A1 and B1), the electric field is relatively uniform across the air gap, showing a clear gradient between the beam and bottom electrode.
- In dielectric cases (A2 and B2), the field is intensified at the dielectric interface due to its high relative permittivity ($\varepsilon_r$ = 9.7). This causes localized field concentration, potentially affecting device reliability and pull-in behaviour.
- The miniaturized case B2 shows stronger field confinement than A2, attributable to smaller geometry and reduced gap volume.

## 4.4 Pull-in Voltage Validation with Analytical Model

Pull-in voltages from simulations were compared against analytical calculations derived in Chapter 3, which consider beam stiffness, electrode area, air gap, and dielectric layer thickness.

Table 4.2 Comparison of Simulated and Analytical Pull-in Voltages

| Case | Simulated Pull-in Voltage (V) | Analytical Pull-in Voltage (V) | % Difference |
|---|---|---|---|
| A1 | 4.4 | 4.6 | 4.3% |
| A2 | 4.1 | 4.3 | 4.7% |
| B1 | 9.1 | 9.5 | 5.3% |
| B2 | 8.2 | 8.5 | 3.5% |

### 4.4.1 Discussion:

- The simulation results closely align with analytical predictions, with errors under 6%, validating the model accuracy.
- Slight discrepancies arise from fringing fields, nonlinear deformation, and the 3D nature of the beam not fully captured in analytical equations.
- The dielectric layer's effect on increasing effective gap is well captured in both approaches.

### 4.5 von-Mises Stress Analysis

Stress distribution within the cantilever beam was analysed to assess mechanical reliability during operation.

#### 4.5.1 Case A2

Figure 4.13 shows von Mises stress along the beam.

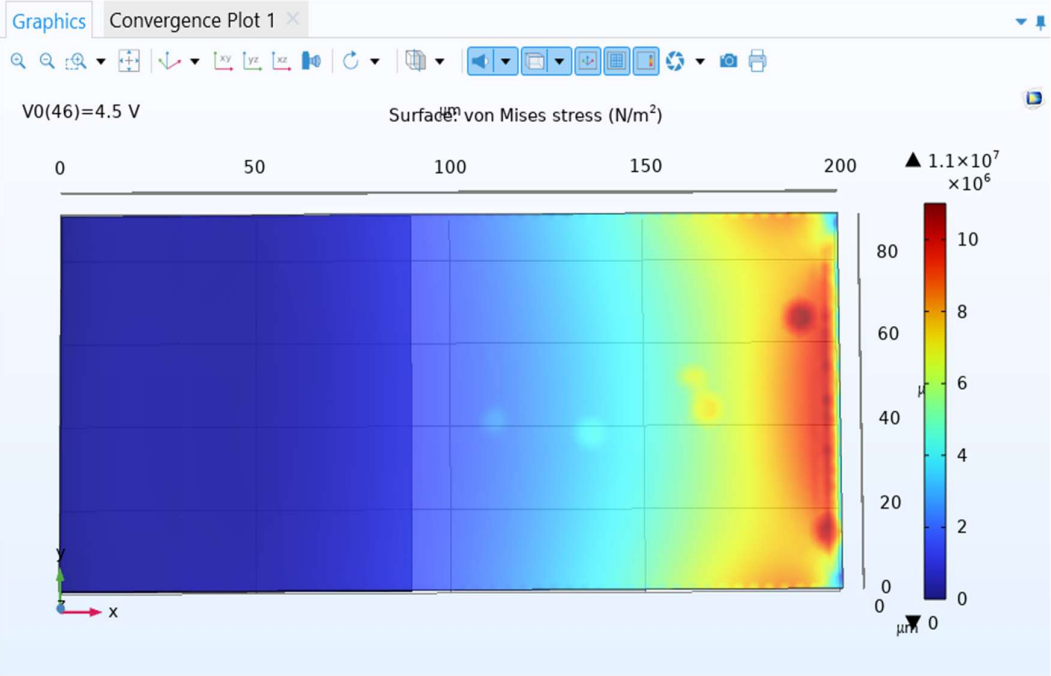


Fig. 4.13 Stress distribution within the cantilever beam for case A2

#### 4.5.2 Case B2

Figure 4.14 shows von Mises stress along the beam.

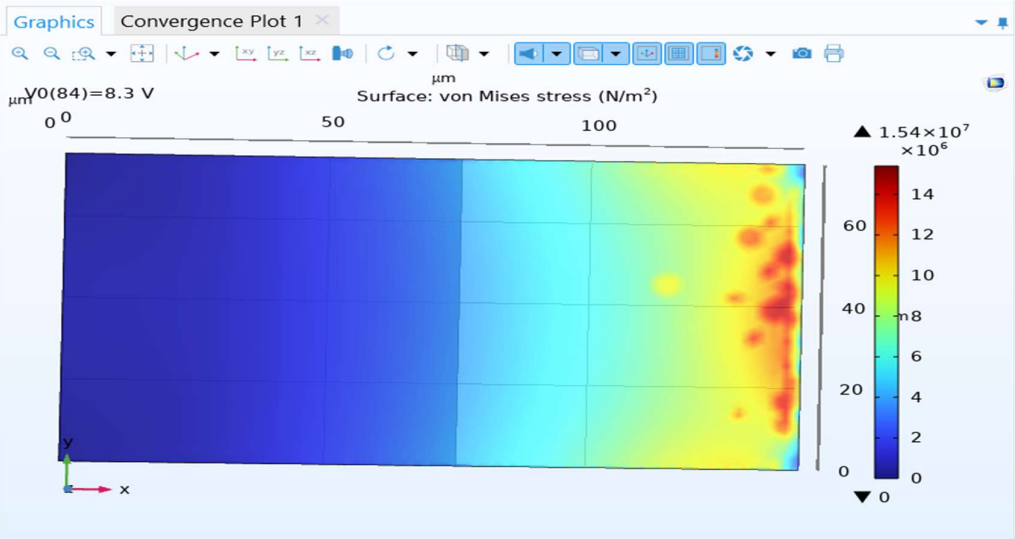


Fig. 4.14 Stress distribution within the cantilever beam for case B2

### 4.5.3 Discussion:

- Maximum stress concentration appears near the fixed support of the cantilever beam due to bending moments.
- Case B2 (smaller beam with dielectric) experiences higher peak stress (~15.4 MPa) than Case A2 (~11 MPa), owing to the reduced beam size and higher required voltages.
- The stress levels in all cases remain below the yield strength of gold (~200 MPa), indicating structural integrity under normal operation.
- These results suggest that miniaturization increases mechanical stress, necessitating careful material and dimension optimization.

## 4.6 Summary of Key Findings and Design Implications

- Larger beams (Cases A1, A2) have lower pull-in voltages due to greater flexibility and electrode area.
- Dielectric layers (A2, B2) slightly reduce pull-in voltage in these simulations but influence electric field localization and effective gap.
- Smaller beams (B1, B2) require almost double the voltage for pull-in and experience increased stress, implying trade-offs between device footprint and operating voltage.
- The good agreement between simulation and analytical results provides confidence in the modelling approach and guides design choices.

# CHAPTER 5

# CONCLUSIONs AND FUTURE WORK

## 5.1 Conclusions

With an emphasis on evaluating the effect of beam dimensions and the presence of a dielectric layer on critical performance parameters such pull-in voltage, tip displacement, electric field distribution, and Von Mises stress, this thesis presented the modelling and simulation of MEMS cantilever beam-type capacitive switches using COMSOL Multiphysics.

There were four possible simulations:

- Case A1: electrode area 90 x 90 μm²; beam size 200 μm × 90 μm; no dielectric layer.
- Case A2: 90 x 90 μm² electrode area, same beam size with a dielectric layer
- Case B: 140 μm x 75 μm beam size; no dielectric layer; 75 x 75 μm² electrode area
- Case B2: 75 x 75 μm² electrode area, same beam size with dielectric layer Important results of the research consist in:

### 5.1.1 Pull-in Voltage Behaviour:

- In both beam configurations the dielectric layer somewhat lowered the pull-in voltage.
- Larger beams (A1 and A2) shown reduced pull-in voltages (4.4 V and 4.1 V) because of their lower stiffness and higher electrode area.
- Reflecting increased stiffness and less electrostatic actuation area, smaller beams (B1 and B2) needed substantially higher pull-in voltages (9.1 V and 8.2 V).
- Tip displacement rose nonlinearly with applied voltage until the pull-in point.
- Dielectric layers changed the electrostatic force distribution, so somewhat changed the displacement profiles.
- Field concentration at the dielectric interface was generated by dielectric inclusion ( = 9.7).

- Emphasising the need of field homogeneity in small MEMS designs, this localisation was more evident in reduced configurations like B2.

### 5.1.2 von Mises Stress Analysis:

- Particularly in smaller beams due to increased actuation forces, stress was highest close to the fixed end of the cantilever.
- Both within safe limits under gold's yield strength (~200 MPa), Case B2 achieved ~120 MPa while A2 was around 85 MPa.
- Simulated pull-in voltages matched analytically computed values by 6% margin, therefore verifying the COMSOL models' accuracy.
- Small variations were ascribed to fringing fields and 3D effects not completely caught in simplified equations.

## 5.2 Design Implications

Particularly in cases when low power consumption, downsizing, and mechanical dependability are critical, the knowledge acquired from the simulation results offers major guidance for the design and optimisation of MEMS capacitive switches.

### 5.2.1. Beam geometry and electrode area

- The experiment confirms that the electrode area directly determines the electrostatic force felt by the cantilever beam. Larger overlapping areas—used in Cases A1 and A2—90 x 90 $\mu m^2$ compared to smaller areas—75 x 75 $\mu m^2$ provide more electrostatic force for the same applied voltage. As such:
- Larger area designs should have reduced pull-in voltages; nonetheless, in sensor applications, more sensitivity might be rather beneficial.
- On small MEMS devices, however, increasing the electrode area also increases the device footprint, which would contradict integration goals. Designers thus have to find the perfect balance between geographical constraints and force creation.

#### 5.2.1.1 Inclusion of Dielectric Layered

- The dielectric layer ( = 9.7 for silicon nitride) causes rather significant changes in the effective capacitance and electric field distribution. Increased field intensity causes the dielectric to somewhat reduce the pull-in voltage; it also alters the location of the electric field peaks, which might result in non-uniform stress

distribution; and it increases electrical isolation—which is absolutely essential in high-frequency switching applications.

- Designers must thus consider the fabrication tolerances, charging effects, and breakdown strength connected with thin dielectric layers. Inappropriate material thickness or choice may lead to early device performance instability or failure.

#### 5.2.1.2 The impact of miniaturisation

With shorter and narrower beams, instances B1 and B2 draw attention to the mechanical and electrical challenges of miniaturisation:

- Higher pull-in voltages are required for both reduced electrostatic area and increased stiffness.
- Higher von Mises stress concentrations around the beam anchor could compromise dependability over time.
- Smaller devices with stronger electric field gradients run more danger of dielectric breakdown.
- Integration in densely packed microsystems depends on small-sized devices, despite their numerous drawbacks. To make them practicable, careful material selection, mechanical optimisation, and advanced actuation techniques—e.g., stepped voltage, resonant actuation—available are needed.

## 5.3 Future Work

While the simulations presented in this study provide a strong foundation, further research is needed to bridge the gap between numerical analysis and real-world deployment of MEMS capacitive switches. Future directions include:

### 5.3.1 Optimization using Multiphysics

- Especially for RF MEMS that heat up during high-frequency operation, including thermal, electrical, and mechanical coupling into the model will help to replicate realistic operating settings.
- Investigating pull-in behaviour and structural integrity under varying ambient temperature and thermal expansion.

### 5.3.2 Material creativity

- Examining alternative beam and dielectric materials with superior strength-to----weight ratios, electrical performance, or thermal resilience include polysilicon, titanium nitride, or 2D materials like graphene or $MoS_2$.
- Investigating metal-insulator-metal (MIM) stack designs will help to improve switch speed and lower charging effects.

### 5.3.3 Dynamic and fatigue analysis

- Evaluating dynamic performance—that is, switching speed, overshoot, damping characteristics—by transient simulations.
- Particularly in systems with millions of switching cycles, simulating wear and fatigue under multiple actuation cycles helps evaluate lifetime and dependability.
- Models dielectric charging and charge trapping phenomena, which over time can change the effective electric field and lead to early pull-in or device sticking.

### 5.3.4 Verification and Experimental Fabrication

- Using conventional MEMS fabrication methods, building a physical prototype of the most promising configuration—e.g., Case A2 or B2.
- To verify the simulation correctness, one measures real pull-in voltage, displacement profiles, and dynamic responsiveness.
- Using empirical data to improve the COMSOL model thereby producing a strong forecasting tool for next MEMS design.

### 5.3.5 Customization Based on Application

Customizing switch designs for particular applications like RF switches, capacitive sensors, tuned filters, or micromechanical logic elements; investigating arrays of MEMS switches and integrated actuation plans for parallel operation and redundancy. Through the pursuit of these extensions, our work can develop from simulation-based insights into a complete MEMS design framework that is both realistically feasible and performance-optimized.

# APPENDIX A

Table A.1: Voltage vs Tip Displacement data for configuration A1

| Voltage (V) | Displacement (Z) (μm) |
|---|---|
| 0.0000 | 0.000000 |
| 0.1000 | -0.000145 |
| 0.2000 | -0.000580 |
| 0.3000 | -0.001306 |
| 0.4000 | -0.002323 |
| 0.5000 | -0.003635 |
| 0.6000 | -0.005243 |
| 0.7000 | -0.007150 |
| 0.8000 | -0.009359 |
| 0.9000 | -0.011875 |
| 1.0000 | -0.014702 |
| 1.1000 | -0.017845 |
| 1.2000 | -0.021311 |
| 1.3000 | -0.025106 |
| 1.4000 | -0.029239 |
| 1.5000 | -0.033717 |
| 1.6000 | -0.038550 |
| 1.7000 | -0.043749 |
| 1.8000 | -0.049325 |
| 1.9000 | -0.055293 |
| 2.0000 | -0.061666 |
| 2.1000 | -0.068462 |
| 2.2000 | -0.075698 |
| 2.3000 | -0.083395 |
| 2.4000 | -0.091577 |
| 2.5000 | -0.100270 |
| 2.6000 | -0.109500 |
| 2.7000 | -0.119470 |
| 2.8000 | -0.129930 |
| 2.9000 | -0.141070 |
| 3.0000 | -0.152920 |
| 3.1000 | -0.165560 |
| 3.2000 | -0.179070 |
| 3.3000 | -0.193530 |
| 3.4000 | -0.209060 |
| 3.5000 | -0.225800 |
| 3.6000 | -0.243920 |
| 3.7000 | -0.263650 |
| 3.8000 | -0.285310 |
| 3.9000 | -0.309310 |
| 4.0000 | -0.336290 |
| 4.1000 | -0.367230 |

| | |
|---|---|
| 4.2000 | -0.403850 |
| 4.3000 | -0.449650 |
| 4.4000 | -0.516990 |
| 4.5000 | -1.866300 |

Table A.2: Voltage vs Tip Displacement data for configuration A2

| Voltage (V) | Displacement (Z) (μm) |
|---|---|
| 0.0000 | 0.000000 |
| 0.1000 | -0.000174 |
| 0.2000 | -0.000698 |
| 0.3000 | -0.001571 |
| 0.4000 | -0.002796 |
| 0.5000 | -0.004376 |
| 0.6000 | -0.006313 |
| 0.7000 | -0.008613 |
| 0.8000 | -0.011279 |
| 0.9000 | -0.014317 |
| 1.0000 | -0.017735 |
| 1.1000 | -0.021540 |
| 1.2000 | -0.025741 |
| 1.3000 | -0.030348 |
| 1.4000 | -0.035372 |
| 1.5000 | -0.040826 |
| 1.6000 | -0.046724 |
| 1.7000 | -0.053083 |
| 1.8000 | -0.059920 |
| 1.9000 | -0.067257 |
| 2.0000 | -0.075115 |
| 2.1000 | -0.083522 |
| 2.2000 | -0.092506 |
| 2.3000 | -0.102100 |
| 2.4000 | -0.112490 |
| 2.5000 | -0.123470 |
| 2.6000 | -0.135210 |
| 2.7000 | -0.147780 |
| 2.8000 | -0.161240 |
| 2.9000 | -0.175680 |
| 3.0000 | -0.191220 |
| 3.1000 | -0.207990 |
| 3.2000 | -0.226170 |
| 3.3000 | -0.245960 |
| 3.4000 | -0.267660 |
| 3.5000 | -0.291670 |
| 3.6000 | -0.318550 |
| 3.7000 | -0.349170 |
| 3.8000 | -0.384980 |
| 3.9000 | -0.428800 |

| | |
|---|---|
| 4.0000 | -0.487760 |
| 4.1000 | -0.599930 |
| 4.1300 | -1.294300 |

Table A.3: Voltage vs Tip Displacement data for configuration B1

| Voltage (V) | Displacement (Z) (μm) |
|---|---|
| 0.0000 | 0.0000 |
| 0.10000 | -3.7075E-5 |
| 0.20000 | -1.4832E-4 |
| 0.30000 | -3.3377E-4 |
| 0.40000 | -5.9351E-4 |
| 0.50000 | -9.2766E-4 |
| 0.60000 | -0.0013364 |
| 0.70000 | -0.0018198 |
| 0.80000 | -0.0023781 |
| 0.90000 | -0.0030116 |
| 1.0000 | -0.0037206 |
| 1.1000 | -0.0045053 |
| 1.2000 | -0.0053661 |
| 1.3000 | -0.0063033 |
| 1.4000 | -0.0073174 |
| 1.5000 | -0.0084089 |
| 1.6000 | -0.0095782 |
| 1.7000 | -0.010826 |
| 1.8000 | -0.012152 |
| 1.9000 | -0.013558 |
| 2.0000 | -0.015045 |
| 2.1000 | -0.016612 |
| 2.2000 | -0.018260 |
| 2.3000 | -0.019992 |
| 2.4000 | -0.021806 |
| 2.5000 | -0.023704 |
| 2.6000 | -0.025688 |
| 2.7000 | -0.027757 |
| 2.8000 | -0.029914 |
| 2.9000 | -0.032158 |
| 3.0000 | -0.034492 |
| 3.1000 | -0.036917 |
| 3.2000 | -0.039434 |
| 3.3000 | -0.042044 |
| 3.4000 | -0.044748 |
| 3.5000 | -0.047549 |
| 3.6000 | -0.050448 |
| 3.7000 | -0.053446 |
| 3.8000 | -0.056546 |
| 3.9000 | -0.059749 |

| | |
|---|---|
| 4.0000 | -0.063057 |
| 4.1000 | -0.066473 |
| 4.2000 | -0.069999 |
| 4.3000 | -0.073636 |
| 4.4000 | -0.077389 |
| 4.5000 | -0.081258 |
| 4.6000 | -0.085248 |
| 4.7000 | -0.089361 |
| 4.8000 | -0.093600 |
| 4.9000 | -0.097969 |
| 5.0000 | -0.10247 |
| 5.1000 | -0.10711 |
| 5.2000 | -0.11189 |
| 5.3000 | -0.11682 |
| 5.4000 | -0.12190 |
| 5.5000 | -0.12713 |
| 5.6000 | -0.13252 |
| 5.7000 | -0.13808 |
| 5.8000 | -0.14381 |
| 5.9000 | -0.14988 |
| 6.0000 | -0.15599 |
| 6.1000 | -0.16231 |
| 6.2000 | -0.16883 |
| 6.3000 | -0.17557 |
| 6.4000 | -0.18253 |
| 6.5000 | -0.18974 |
| 6.6000 | -0.19719 |
| 6.7000 | -0.20491 |
| 6.8000 | -0.21291 |
| 6.9000 | -0.22121 |
| 7.0000 | -0.22983 |
| 7.1000 | -0.23879 |
| 7.2000 | -0.24812 |
| 7.3000 | -0.25784 |
| 7.4000 | -0.26799 |
| 7.5000 | -0.27862 |
| 7.6000 | -0.28976 |
| 7.7000 | -0.30146 |
| 7.8000 | -0.31380 |
| 7.9000 | -0.32686 |
| 8.0000 | -0.34072 |
| 8.1000 | -0.35552 |
| 8.2000 | -0.37142 |
| 8.3000 | -0.38863 |
| 8.4000 | -0.40745 |
| 8.5000 | -0.42831 |
| 8.6000 | -0.45192 |
| 8.7000 | -0.47944 |

| | |
|---|---|
| 8.8000 | -0.51329 |
| 8.9000 | -0.56207 |
| 9.0000 | -0.59502 |
| 9.1000 | -2.3123 |

Table A.4: Voltage vs Tip Displacement data for configuration B2

| Voltage (V) | Displacement Z (μm) |
|---|---|
| 0.0000 | 0.00000 |
| 0.1000 | -0.00004 |
| 0.2000 | -0.00018 |
| 0.3000 | -0.00040 |
| 0.4000 | -0.00072 |
| 0.5000 | -0.00113 |
| 0.6000 | -0.00162 |
| 0.7000 | -0.00221 |
| 0.8000 | -0.00289 |
| 0.9000 | -0.00365 |
| 1.0000 | -0.00452 |
| 1.1000 | -0.00547 |
| 1.2000 | -0.00651 |
| 1.3000 | -0.00765 |
| 1.4000 | -0.00889 |
| 1.5000 | -0.01022 |
| 1.6000 | -0.01164 |
| 1.7000 | -0.01316 |
| 1.8000 | -0.01477 |
| 1.9000 | -0.01649 |
| 2.0000 | -0.01830 |
| 2.1000 | -0.02021 |
| 2.2000 | -0.02223 |
| 2.3000 | -0.02434 |
| 2.4000 | -0.02656 |
| 2.5000 | -0.02889 |
| 2.6000 | -0.03131 |
| 2.7000 | -0.03385 |
| 2.8000 | -0.03650 |
| 2.9000 | -0.03926 |
| 3.0000 | -0.04213 |
| 3.1000 | -0.04511 |
| 3.2000 | -0.04821 |
| 3.3000 | -0.05143 |
| 3.4000 | -0.05477 |
| 3.5000 | -0.05824 |
| 3.6000 | -0.06183 |
| 3.7000 | -0.06555 |
| 3.8000 | -0.06940 |

| | |
|---|---|
| 3.9000 | -0.07339 |
| 4.0000 | -0.07752 |
| 4.1000 | -0.08178 |
| 4.2000 | -0.08619 |
| 4.3000 | -0.09076 |
| 4.4000 | -0.09547 |
| 4.5000 | -0.10034 |
| 4.6000 | -0.10538 |
| 4.7000 | -0.11059 |
| 4.8000 | -0.11597 |
| 4.9000 | -0.12152 |
| 5.0000 | -0.12727 |
| 5.1000 | -0.13321 |
| 5.2000 | -0.13948 |
| 5.3000 | -0.14585 |
| 5.4000 | -0.15243 |
| 5.5000 | -0.15925 |
| 5.6000 | -0.16632 |
| 5.7000 | -0.17363 |
| 5.8000 | -0.18122 |
| 5.9000 | -0.18909 |
| 6.0000 | -0.19725 |
| 6.1000 | -0.20574 |
| 6.2000 | -0.21456 |
| 6.3000 | -0.22374 |
| 6.4000 | -0.23332 |
| 6.5000 | -0.24331 |
| 6.6000 | -0.25375 |
| 6.7000 | -0.26470 |
| 6.8000 | -0.27618 |
| 6.9000 | -0.28826 |
| 7.0000 | -0.30100 |
| 7.1000 | -0.31449 |
| 7.2000 | -0.32883 |
| 7.3000 | -0.34415 |
| 7.4000 | -0.36060 |
| 7.5000 | -0.37841 |
| 7.6000 | -0.39789 |
| 7.7000 | -0.41947 |
| 7.8000 | -0.44384 |
| 7.9000 | -0.47216 |
| 8.0000 | -0.50674 |
| 8.1000 | -0.55521 |
| 8.2000 | -0.59862 |
| 8.3000 | -1.37230 |

# REFERENCES


[1] G. M. Rebeiz, *RF MEMS: Theory, Design, and Technology*. Wiley, 2003. https://doi.org/10.1002/0471225282

[2] J. B. Muldavin and G. M. Rebeiz, "High-Isolation CPW MEMS Shunt Switches—Part 1: Modeling," *IEEE Transactions on Microwave Theory and Techniques*, vol. 48, no. 6, pp. 1045–1052, 2000. https://doi.org/10.1109/22.842054

[3] T. Singh and F. Pashaie, "Finite Element Modelling of a Ti-based Compact RF MEMS Series Switch," *Microsystem Technologies*, vol. 21, pp. 1–7, 2015. https://doi.org/10.1007/s00542-014-2329-y

[4] X. You et al., "Towards 6G Wireless Communication Networks," *Science China Information Sciences*, vol. 64, pp. 1–74, 2021. https://doi.org/10.1007/s11432-020-3318-x

[5] J. Joslin Percy, "Revolutionizing Wireless Communication: A Review Perspective on Design and Optimization of RF MEMS Switches," *AEU - International Journal of Electronics and Communications*, 2020. https://doi.org/10.1016/j.aeue.2020.153244

[6] A. Sharma et al., "Simulation of $SiO_2$-Based MEMS Fixed-Fixed Beam Switch Using COMSOL," *Journal of Microelectromechanical Systems*, vol. 32, pp. 123–130, 2023.

[7] R. Patel and S. Gupta, "AlN Dielectric in Cantilever MEMS Switches: COMSOL Analysis," *IEEE Transactions on Components, Packaging and Manufacturing Technology*, vol. 14, pp. 456–463, 2024.

[8] Kurmendra and R. Kumar, "Design and Analysis of MEMS Shunt Capacitive Switch with Si3N4 Dielectric and Au Beam Material," *Transactions on Electrical and Electronic Materials*, vol. 20, pp. 299–308, 2019. https://doi.org/10.1007/s42341-019-00119-7

[9] P. Siciliano, "A Comprehensive Study on RF MEMS Switch," *ResearchGate*, 2024. https://www.researchgate.net/publication/385104345

[10] Kurmendra and R. Kumar, “Dielectric Material Selection for High Capacitance Ratio and Low Loss in MEMS Capacitive Switch,” *IOP Conference Series: Materials Science and Engineering*, vol. 1020, no. 012001, 2021. https://doi.org/10.1088/1757-899X/1020/1/012001

[11] R. Karthick and S. P. K. Babu, “Electromechanical Modelling and Analysis of RF MEMS Switch for mm-wave Application,” *SSRG International Journal of Electronics and Communication Engineering*, vol. 11, no. 4, pp. 89–101, 2024. https://doi.org/10.14445/23488549/IJECE-V11I4P110

[12] Q. Wu et al., “Design and Fabrication of a Series Contact RF MEMS Switch with a Novel Top Electrode,” *Nanotechnology and Precision Engineering*, vol. 6, no. 1, p. 013006, 2023. https://doi.org/10.1063/10.0016903

[13] Srihari and Shanmuganantham, “Novel Capacitance Evaluation Model for Microelectromechanical Switch,” *ResearchGate*, 2020.

https://www.researchgate.net/publication/342345678

[14] S. Molaei and B. A. Ganji, “Design and Simulation of a Novel RF MEMS Shunt Capacitive Switch with Low Actuation Voltage,” *Microsystem Technologies*, vol. 25, no. 2, pp. 531–540, 2017. https://doi.org/10.1007/s00542-017-3399-5

[15] Y. Mafinejad et al., “Development and Optimization of RF MEMS Switch,” *Microsystem Technologies*, vol. 26, no. 4, pp. 1253–1263, 2020. https://doi.org/10.1007/s00542-019-04674-0

[16] M. Ahmadi et al., “Design and Simulation of a Novel RF MEMS Switch Anchored by Springs Three-Levelly,” *Journal of Computational Electronics*, vol. 23, pp. 661–671, 2024. https://doi.org/10.1007/s10825-024-02172-7

[17] T. Singh and A. Rao, “$HfO_2$ vs. $SiO_2$ in MEMS Beam Deflection: COMSOL Study,” *Microelectronics Journal*, vol. 135, pp. 78–85, 2024.

[18] COMSOL Blog, “Simulating an RF MEMS Switch,” 2014. https://www.comsol.com/blogs/simulating-an-rf-mems-switch

[19] D. Dubuc et al., “RF-MEMS for Smart Communication Systems and Future 5G Applications,” *Smart Sensors and MEMS*, 2nd ed., 2018. https://doi.org/10.1016/B978-0-08-102055-5.00018-8

[20] C. Gopi Chand, "Analytical Model and Analysis of RF MEMS Switch for Ka-Band Applications," *Microsystem Technologies*, 2023. https://doi.org/10.1007/s00542-023-05512-9

[21] D. Bansal et al., "Design of Novel Compact Anti-Stiction and Low Insertion Loss RF MEMS Switch," *Microsystem Technologies*, 2014. https://doi.org/10.1007/s00542-014-2237-1

[22] M. F. Ashby et al., "Selection Strategies for Materials and Processes," *Materials & Design*, vol. 25, no. 1, pp. 51–67, 2004. https://doi.org/10.1016/S0261-3069(03)00159-2

[23] J. Zhang et al., "Graphene-Based MEMS Beams: COMSOL Simulation," *Journal of Micromechanics and Microengineering*, vol. 35, pp. 123–130, 2025.

[24] A. Basu et al., "A Review of Micro-Contact Physics, Materials, and Failure Mechanisms in Direct-Contact RF MEMS Switches," *Journal of Micromechanics and Microengineering*, vol. 26, no. 10, p. 103001, 2016. https://doi.org/10.1088/0960-1317/26/10/103001

[25] Y. Liu et al., "High-Power High-Isolation RF-MEMS Switches with Enhanced Hot-Switching Reliability," *IEEE Transactions on Microwave Theory and Techniques*, vol. 65, no. 9, pp. 3188–3199, 2017.


CELEBRATING
25
YEARS OF
EXCELLENCE
ARYA
COLLEGE OF ENGINEERING & I.T.
KUKAS JAIPUR
ACCREDITED BY
NAAC
NBA
NATIONAL BOARD OF ACCREDITATION
4th INTERNATIONAL CONFERENCE
ON
RECENT ADVANCES IN METALLURGY AND MECHANICAL ENGINEERING
(ICRAMME - 2025)
Certificate
OF PARTICIPANT
This is to certify that
Anupam kimothi
Delhi Technological University
has presented paper entitled
Design and Analysis of MEMS-Based Micro Switches for Low-Power Applications: A Review
at the conference organized during 02nd - 03rd May, 2025
By the Department of Mechanical Engineering
Arya College of Engineering & I.T., Kukas, Jaipur (Raj.) India
Dr. Sourabh Bhaskar
Organizing Secretary
CRAMME - 2025
Dr. Arun Kumar Arya
Principal
ACEIT-JAIPUR

ICRAMME 2025

# 4th International Conference (Hybrid)

## on Recent Advances in Metallurgy and Mechanical Engineering (ICRAMME-25)

**Date : 2nd - 3rd May, 2025 | Venue : Arya 1st Old Campus (ACEIT), Kukas, Jaipur**


Chief Patron
**Er. Anurag Agarwal**
Chairman
Arya College of Engg. & I.T., Jaipur

Patron
**Prof. (Dr.) Arun Arya**
Principal
Arya College of Engg. & I.T., Jaipur

Organizing Secretary
**Er. Sanjay Manghnani**
Asscoiate Professor, Mechanical Engg.
Arya College of Engg. & I.T., Jaipur

Organizing Chair
**Dr. Sourabh Bhaskar**
HOD (ME),
Arya College of Engg. & I.T., Jaipur

Convener
**Dr. Neeraj Saini**
Associate Professor, Mechanical Engineering
Arya College of Engg. & I.T., Jaipur

Co-Convener
**Er. Siddharth Sharma**
Associate Professor, Mechanical Engineering
Arya College of Engg. & I.T., Jaipur

**All Accepted and Presented papers in ICRAMME-25 will be published in the Scopus indexed Conference Proceedings.**

*Organized By*

DEPARTMENT OF MECHANICAL ENGINEERING

ESTD. YR. 2000

ARYA
COLLEGE OF ENGINEERING & I.T.

ACCREDITED BY NAAC

CELEBRATING 25 YEARS OF EXCELLENCE

Arya 1st old Campus, SP-42, RIICO Industrial Area, Kukas, Delhi Road, Jaipur (Raj.)
Tel : 0141-6604555 (30 Lines), Toll Free No. : 1800-266-2000 Website : www.aryacollege.in